Published in final edited form as:
Amino Acids. 2012 January ; 42(1): 95–113. doi:10.1007/s00726-010-0603-6.

Design of Mn porphyrins for treating oxidative stress injuries and their redox-based regulation of cellular transcriptional activities

Ines Batinic-Haberle,
Department of Radiation Oncology, Duke University Medical Center, 281b/285 MSRB I, Durham, NC 27710, USA

Ivan Spasojevic,
Department of Medicine, Duke University Medical Center, Durham, NC 27710, USA

Hubert M. Tse,
Department of Microbiology, Comprehensive Diabetes Center Birmingham, University of Alabama at Birmingham, Birmingham, AL 35294, USA

Artak Tovmasyan,
Department of Radiation Oncology, Duke University Medical Center, 281b/285 MSRB I, Durham, NC 27710, USA

Zrinka Rajic,
Department of Radiation Oncology, Duke University Medical Center, 281b/285 MSRB I, Durham, NC 27710, USA

Daret K. St. Clair,
Graduate Center for Toxicology, University of Kentucky, Lexington, KY 40536, USA

Zeljko Vujaskovic,
Department of Radiation Oncology, Duke University Medical Center, 281b/285 MSRB I, Durham, NC 27710, USA

Mark W. Dewhirst, and
Department of Radiation Oncology, Duke University Medical Center, 281b/285 MSRB I, Durham, NC 27710, USA

Jon D. Piganelli
Children's Hospital, Rangos Research Center, University of Pittsburgh, Pittsburgh, PA 15213, USA

Ines Batinic-Haberle: ibatinic@duke.edu

Abstract

The most efficacious Mn(III) porphyrinic (MnPs) scavengers of reactive species have positive charges close to the Mn site, whereby they afford thermodynamic and electrostatic facilitation for the reaction with negatively charged species such as $O_2^{\bullet -}$ and $ONOO^-$. Those are Mn(III) *meso* tetrakis(*N*-alkylpyridinium-2-yl)porphyrins, more specifically MnTE-2-PyP^{5+} (AEOL10113) and MnTnHex-2-PyP^{5+} (where alkyls are ethyl and *n*-hexyl, respectively), and their imidazolium analog, MnTDE-2-ImP^{5+} (AEOL10150, Mn(III) *meso* tetrakis(*N*,*N*′-diethylimidazolium-2-yl) porphyrin). The efficacy of MnPs in vivo is determined not only by the compound antioxidant potency, but also by its bio-availability. The former is greatly affected by the lipophilicity, size,

Correspondence to: Ines Batinic-Haberle, ibatinic@duke.edu.

structure, and overall shape of the compound. These porphyrins have the ability to both eliminate reactive oxygen species and impact the progression of oxidative stress-dependent signaling events. This will effectively lead to the regulation of redox-dependent transcription factors and the suppression of secondary inflammatory- and oxidative stress-mediated immune responses. We have reported on the inhibition of major transcription factors HIF-1α, AP-1, SP-1, and NF-κB by Mn porphyrins. While the prevailing mechanistic view of the suppression of transcription factors activation is via antioxidative action (presumably in cytosol), the pro-oxidative action of MnPs in suppressing NF-κB activation in nucleus has been substantiated. The magnitude of the effect is dependent upon the electrostatic (porphyrin charges) and thermodynamic factors (porphyrin redox ability). The pro-oxidative action of MnPs has been suggested to contribute at least in part to the in vitro anticancer action of MnTE-2-PyP^{5+} in the presence of ascorbate, and in vivo when combined with chemotherapy of lymphoma. Given the remarkable therapeutic potential of metalloporphyrins, future studies are warranted to further our understanding of in vivo action/s of Mn porphyrins, particularly with respect to their subcellular distribution.

Keywords

SOD mimics; Peroxynitrite scavengers; Mn porphyrins; Cellular transcriptional activity; MnTE-2-PyP^{5+}; MnTnHex-2-PyP^{5+}; NF-κB

Introduction

The increased knowledge of the impact of normal cellular redox status, i.e. the balance between the endogenous antioxidant systems and reactive oxygen (ROS) and nitrogen (RNS) species, on cell function (Halliwell and Gutteridge 2007; Jones 2008; Trachootham et al. 2009; McCord 2000) has been accompanied by the need to restore it under pathological conditions. Several types of synthetic antioxidants as well as natural antioxidants have been employed in different models of oxidative stress injuries such as ischemia/reperfusion, radiation, cancer, diabetes, aging, injuries of central nervous systems, etc. We recently summarized the ROS/RNS-related chemistry as well as in vivo effects of several major groups of synthetic SOD mimics (Batinic-Haberle et al. 2010). Herein, we addressed the design and development of the most potent and bioavailable Mn porphyrin-based therapeutics and their role in redox-based cellular signaling pathways.

The ability of Mn porphyrins and other potent synthetic and endogenous antioxidants to easily donate and accept electrons allows them to exert both anti- and pro-oxidative activities. Both the lack of ROS/RNS and their excessive formation have been known to dysregulate cellular metabolism (McCord 2008). The anti-oxidative action of Mn porphyrins has been well substantiated and proven beneficial. However, the pro-oxidative action/s may be therapeutically beneficial as well. Several published reports provided experimental evidences that imply the pro-oxidative mode of action of MnPs with respect to (1) suppression of transcription factors activation (Tse et al. 2004) and (2) tumor killing (Jaramillo et al. 2009; Ye et al. 2009; Spasojevic et al. 2006). Understanding the action/s of MnPs (and other classes of antioxidants) remains a challenge.

Design of Mn porphyrins with respect to their ability to dismute $O_2^{\bullet -}$

The most obvious approach to the design of potent SOD mimics has been to mimic the electrostatic and thermodynamic properties of the SOD enzyme. Thus, such compounds should catalyze the $O_2^{\bullet -}$ dismutation (Eqs. 1 and 2) around the metal-centered reduction potential of the SOD enzyme: $E_{1/2}$ of ~+300 mV versus NHE. This is the midway potential

between the potential for the reduction (+890 mV vs. NHE) and oxidation of $O_2^{\bullet-}$ (−160 mV vs. NHE); therefore, the enzyme reduces and oxidizes $O_2^{\bullet-}$ with identical rate constants of 2×10^9 M^{-1} s^{-1} (Fig. 1) (Klug-Roth et al. 1973; Vance and Miller 1998; Michel et al. 2005; Goldstein et al. 2006). The remarkable contribution of the electrostatics to the $O_2^{\bullet-}$ dismutation that allows the enzyme to operate at diffusion limited rates will be addressed further below. The unsubstituted Mn porphyrins (such as MnT-2(or 4)-PyP^+ and $MnTPP^+$) have $E_{1/2}$ for $Mn^{III}P/Mn^{II}P$ redox couple of ~−300 mV versus NHE (Fig. 1; Table 1) (Batinic-Haberle et al. 2010), and thus have Mn stabilized in +3 oxidation state and cannot be reduced in the first step by $O_2^{\bullet-}$ (Eq. 1). Moreover, the substituted porphyrins that bear negative charges ($MnTBAP^{3-}$ and $MnTSPP^{3-}$), and no charges at the periphery ($MnhematoP^-$), with $E_{1/2}$ ~ −200 mV versus NHE (Batinic-Haberle et al. 2010) cannot be reduced with $O_2^{\bullet-}$. In order to increase the reducibility of Mn site, i.e. the affinity of MnPs for electrons, the metal center must be made electron-deficient

$$Mn^{III}P^+ + O_2^{\bullet-} \iff MN^{II}P + O_2 \quad (1)$$

$$Mn^{II}P + 2\,H^+ + O_2^{\bullet-} \iff Mn^{III}P^+ + H_2O_2 \quad (2)$$

electron-withdrawing groups attached to the porphyrin *meso* and/or to *beta* pyrrolic positions. The unlimited possibilities of porphyrin modifications at *meso* and *beta* positions allowed us to modify metal-centered reduction potential within 1 V range (Fig. 1). The very first compound of reasonable SOD-like activity, $FeTM\text{-}4\text{-}PyP^{5+}$, was characterized by Pasternack and Halliwell (1979). The porphyrin is substituted with electron-withdrawing positively charged pyridyl *meso* substituents. The cationic nitrogens are placed in *para* (4) positions on pyridyls with respect to *meso* porphyrinic positions (Figs. 1, 2).

Later, Mn analog, $MnTM\text{-}4\text{-}PyP^{5+}$ was also studied (Peretz et al. 1982; Lee et al. 1998). However, both compounds are of highly planar structure (Koner and Goldberg 2009). Thus their positive charges are exposed and allow the porphyrin to associate with anionic phosphates of nucleic acids in vivo, which in turn imposes toxicity and loss of SOD-like activity (Fig. 2)(Batinic-Haberle et al. 1998). To reduce their affinity for nucleic acids, their bulkiness was increased by moving methyl groups from *para* (4) onto *ortho* (2) positions (Fig. 2) (Batinic-Haberle et al. 1998). Due to the crowding between the *meso N*-pyridyl alkyls and *β*-pyrrolic hydrogens, alkylpyridyl groups of *ortho* isomers cannot rotate freely, but are stuck in a position vertical to the porphyrin plane. As a result of the increased bulkiness, charges are shielded and the *ortho* isomer does not associate with nucleic acids, and thus, does not lose SOD-like activity in vivo as was shown in *E. coli* studies (Batinic-Haberle et al. 1998). Importantly, placement of alkyl groups on *ortho* positions afforded additional increase in Mn electron-deficiency, and enhanced electrostatic attraction of superoxide and peroxynitrite to the Mn site (see below). The *ortho* isomer, $MnTM\text{-}2\text{-}PyP^{5+}$ has the $E_{1/2}$ = +220 mV versus NHE, very similar to the $E_{1/2}$ of the enzyme. Consequently, it has high k_{cat} of 5.8×10^7 M^{-1} s^{-1} (Batinic-Haberle et al. 1998). Several other *meso* pyridyl porphyrins were synthesized having $E_{1/2}$ ~ +300 mV versus NHE (Batinic-Haberle et al. 2002, 2004, 2006). We also synthesized Mn porphyrins that have both *meso* and *beta* electron-withdrawing substituents. In such compounds the charges on *meso* substituents are maintained to afford favorable electrostatics and $E_{1/2}$ was further increased; thus, they are the most potent SOD mimics, and “sit” in the plateau region of the bell-shape curve of the structure–activity relationship (Fig. 3). With eight bromines in all *beta* positions, and *meso*

meta N-methylpyridyl groups, $MnBr_8TM\text{-}3\text{-}PyP^{4+}$, has $E_{1/2}$ of +460 mV versus NHE, and is the most potent SOD mimic thus far synthesized, with k_{cat} identical to the k_{cat} of the SOD enzyme (DeFreitas-Silva et al. 2008) (Fig. 2; Table 1). Yet, such high positive $E_{1/2}$ stabilized the Mn +2 oxidation state to such extent that the compound exists as a Mn(II) porphyrin. In turn, it is insufficiently stable in solution, easily loses metal, and therefore, ceases to be an SOD mimic. While excellent mechanistic tools in designing SOD mimic, such MnPs are of no practical importance as therapeutics. As compared to other types of antioxidants, most potent Mn porphyrins, particularly our lead compounds, *meso* substituted $MnTE\text{-}2\text{-}PyP^{5+}$ and $MnTnHex\text{-}2\text{-}PyP^{5+}$, are extremely stable under all conditions of acidity, dilution, temperature, and light.

Some of our compounds, such as $MnBr_8TSPP^{3-}$ (Rebouças et al. 2008a, b, c) (Fig. 2; Table 1), and members of other classes of synthetic antioxidants such as $Mn(salens)^{+}$ and Mn cyclic polyamines possibly act as transporters of Mn into the cell and its compartments. Mn low molecular weight complexes possess fair SOD-like activity, and can under certain conditions protect against ROS/RNS-mediated injury (Batinic-Haberle et al. 2010 and refs therein).

A number of Mn porphyrins were analyzed, and structure–activity relationship (SAR), which relates the log k_{cat} to $E_{1/2}$, was established (Fig. 3). It encompasses compounds of different electrostatics and stericity (Batinic-Haberle et al. 1999). The SAR showed that higher (the more positive) $E_{1/2}$ gives rise to the higher k_{cat}. At very low potentials, $E_{1/2} \ll$ +200 mV versus NHE, the $Mn^{III}Ps$ are stabilized in their +3 oxidation state, and their reduction to $Mn^{II}P$ (eq [1]) is a rate limiting step (raising limb of SAR). With the increase in $E_{1/2}$, the reduction of $Mn^{III}P$ becomes easier, and thus k_{cat} increases. Alike enzyme, with $MnTE\text{-}2\text{-}PyP^{5+}$ at +228 mV versus NHE, the rate constants for both steps of dismutation process, oxidation and reduction of MnP with $O_2^{\bullet -}$ are similar, $2.5 \times 10^7\ M^{-1}\ s^{-1}$ and $8.2 \times 10^7\ M^{-1}\ s^{-1}$, respectively (Batinic-Haberle et al. 2004). At the potentials around +500 mV, the maximal k_{cat} was achieved. As the $E_{1/2}$ increases further beyond +500 mV, the electron-deficiency of the metal site increases so much that eventually Mn(II) porphyrin becomes a stable species in solution, and the oxidation of $Mn^{II}P$ to $Mn^{III}P$ (Eq. 2) becomes a rate-limiting step (falling limb of SAR). Consequently, k_{cat} starts to drop again (Batinic-Haberle et al. 2002,2010).

We have recently showed that there is a remarkable ~100-fold increase in the k_{cat} of cationic versus those porphyrins that have either no charges or negative charges on the periphery (Batinic-Haberle et al. 2010). As expected, in the latter case, due to the repulsion of anionic superoxide from anionic porphyrin, the effect was larger than with neutral compounds. The effect of the charges on the k_{cat} of MnPs is similar in magnitude to the effect established with the enzyme itself (Spasojevic et al. 2003 and refs therein). The high k_{cat} of the enzyme suggests a diffusion-limited process; the crystal structure showed that the positively charged amino acids provide a tunnel to guide anionic superoxide to the metal site. Recently, with the wealth of data on numerous MnPs we established the individual SARs for cationic, anionic, and neutral porphyrins (Rebouças et al. 2009), accounting for the electrostatic effects. Such SARs show that, for any given $E_{1/2}$, the k_{cat} is the highest for the cationic porphyrins and most so for those compounds which have positive charges closer to the Mn site, i.e. *ortho* isomeric substituted pyridylporphyrins (Rebouças et al. 2009). Based on SAR, the *ortho* isomeric Mn(III) tetrakis(*N*-alkylpyridinium-2-yl)porphyrins (Figs. 2, 3; Table 1) were identified as the most potent compounds. The ethyl analog, $MnTE\text{-}2\text{-}PyP^{5+}$ (Fig. 2), was forwarded to in vitro and in vivo studies.

The reactivity toward other ROS/RNS

In collaboration with Rafael Radi and Gerardo Ferrer-Sueta, the reactivity of *ortho* Mn(III) *N*-alkylpyridylporphyrins toward $ONOO^-$ was determined to parallel their ability to dismute $O_2^{\bullet -}$, making them the most potent synthetic scavengers of peroxynitrite also (Table 1) (Ferrer-Sueta et al. 2003;Ferrer-Sueta and Radi 2009). Carnieri et al. have reported the high potency of *para* isomer, MnTM-4-PyP^{5+}, in reducing hypochlorous acid, HClO, which is produced by myeloperoxidase during inflammation (Halliwell and Gutteridge 2007). Given the fact that HClO is able to oxidize MnP in a manner similar to $ONOO^-$ (Carnieri et al. 1982;Ferrer-Sueta et al. 2003), and that *ortho* isomer of Mn(III) alkylpyridylporphyrins are more efficacious in reducing $ONOO^-$ than *para* analogs, we would expect MnTM-2-PyP^{5+} to reduce HClO more readily than MnTM-4-PyP^{5+}. The reactivity toward HClO just adds to the wide spectrum of the species that MnPs may eliminate, which in turn challenges us with the complexity of reactions and mechanisms of action(s) of this and other synthetic antioxidants. Further, MnPs react readily with cellular reductants: ascorbate, glutathione, uric acid, and tetrahydrobiopterin (Ferrer-Sueta et al. 1999,2006;Batinic-Haberle et al. 2004). They can be also reduced with cellular flavoenzymes (Ferrer-Sueta et al. 2006;Kachadourian et al. 2004) and thioredoxin reductase (Faulkner et al. 1994) as well as by nitric oxide (Spasojevic et al. 2000;Pfeiffer et al. 1998). Thus, in vivo, in a first step of MnP-based catalysis of $O_2^{\bullet -}$ dismutation, $Mn^{III}P$ would likely be reduced to $Mn^{II}P$ with cellular reductants, and not with $O_2^{\bullet -}$. Also the reduction of $ONOO^-$ by MnP may be coupled to cellular reductants. In a first step, $Mn^{III}P$ could be reduced to $Mn^{II}P$. In a second step, $Mn^{II}P$ would react two-electronically with $ONOO^-$, whereby $O=Mn^{IV}P$ and benign NO_2^- would be formed. The highly reactive, high-valent Mn(IV) species, $O=Mn^{IV}P$ could then be reduced back to a stable Mn +3 oxidation state with either uric acid, or ascorbic acid or glutathione, whereby sparing biological molecules (Ferrer-Sueta et al. 1999).

Design of Mn porphyrins with respect to their bioavailability

For a while the prevailed opinion had been that the excessively charged compounds cannot accumulate to a high extent in important cellular compartments, particularly in mitochondria. Most recently, several groups have designed compounds that target mitochondria due to their critical role in normal cell functioning. Murphy (2008) developed a concept that in addition to a redox-able unit (ubiquinone, nitroxide, vitamin E, ebselen, etc.), the compound must be positively charged and of appropriate lipophilicity in order to reach mitochondria. Based on such concept, we hypothesized that our cationic MnPs would accumulate in mitochondria. For that purpose we developed HPLC/fluorescence and LC-MS/MS methods to determine MnTE-2-PyP^{5+} and its analogs in vivo (Spasojevic et al. 2007, 2008). In a study by Ferrer-Sueta et al. (2006), ≥3 μM MnTE-2-PyP^{5+} was able to protect submitochondrial particles against $ONOO^-$ flux. In a following study we found that MnTE-2-PyP^{5+} reaches mouse heart mitochondria at levels high enough (5.1 μM) to protect it against $ONOO^-$-mediated damage (Spasojevic et al. 2007). Preliminary data already indicate higher mouse heart mitochondrial accumulation of MnTnHex-2-PyP^{5+} as compared to hydrophilic MnTE-2-PyP^{5+} (Spasojevic et al., unpublished). We further found that MnTE-2-PyP^{5+} accumulates in nucleus of macrophages at threefold higher levels than in cytosol, presumably driven there by the negatively charged phosphates of nucleic acids (Fig. 8b).

We have obviously achieved the maximal antioxidant potency of MnP in aqueous systems (k_{cat}) as discussed above (plateau in Fig. 3). We can further enhance the in vivo effects by increasing the availability of potent Mn(III) *N*-substituted pyridylporphyrins, primarily by reducing their excessive hydrophilicity. To do so, we recently developed a method to

quantify the MnP lipophilicity by its partition between *n*-octanol and water (P_{OW}) (Table 1) (Kos et al. 2009b). Such measurements allow us to assess more precisely the MnPs lipophilicity and compare them to other drugs of similar targets. At the present state of our insight into the structure and in vivo actions of MnPs, the lipophilicity of Mn(III) *N*-alkylpyridylporphyrins can be increased tenfold: (1) by lengthening the *meso* alkylpyridyl chains by each additional CH_2 group, or (2) by shifting the alkyl groups from *ortho* onto *meta* (indicated by number 3 in formulas) pyridyl positions (Fig. 2). The first modification does not affect the k_{cat} as the charges are still positioned at the same distance with respect to the Mn site. Thus, MnTM-2-PyP^{5+} and MnTnOct-2-PyP^{5+} are of nearly identical k_{cat} ($O_2^{\bullet-}$) and k_{red} ($ONOO^-$) (Table 1). Second modification places positive charges further away from the Mn site, and thus, causes the decrease in SOD-like activity. The *meta* isomeric compounds are still bulky enough, and thus, do not associate significantly with nucleic acids and are not toxic when compared to *para* analogs.

In vivo and in vitro effects

The critical role of the MnP bioavailability

Most of the in vitro and in vivo effects have been recently summarized in Batinic-Haberle et al. 2010. Herein, we pointed out in particular those studies which clearly addressed the critical importance of lipophilicity for in vivo efficacy of MnPs.

The effect of the length of alkyl chains on meso pyridyl substituents—The up to 120-fold increased efficacy of MnTnHex-2-PyP^{5+} in vivo when compared to MnTE-2-PyP^{5+} (Saba et al. 2007; Batinic-Haberle et al. 2009b) (Table 1) is due to its 13,500-fold increased lipophilicity (Kos et al. 2009b) (Table 1) and 12-fold higher ability to cross blood brain barrier (Doyle et al. 2009). In a rat renal ischemia/reper-fusion model, single *iv* injection of only 50 μg of MnTn-Hex-2-PyP^{5+} protected against ATP depletion, MnSOD inactivation, protein 3-nitrotyrosine formation, and renal dysfunction (Saba et al. 2007). In a rat stroke 90-min middle cerebral artery occlusion model, due to the 12-fold higher ability to cross blood brain barrier (Doyle et al. 2009), MnTnHex-2-PyP^{5+} decreased stroke volume and neurologic deficit when 450 μg/kg/day was given intravenously for a week, starting at 90 min after reperfusion (Warner et al. 2010) (of note, previous data show that MnP delivery as late as 6 h after reperfusion still reduces infarct size significantly; Mackensen et al. 2001). In a rabbit cerebral palsy model, MnTnHex-2-PyP^{5+} rescued rabbit puppies, but MnTE-2-PyP^{5+} did not (Yu et al. 2010). Mn porphyrins were given to a rabbit dam twice, 30 min before and 30 min after the 40-min uterus ischemia at 0.1 and 1 mg/kg (MnTnHex-2-PyP^{5+}) and 6 mg/kg (MnTE-2-PyP^{5+}). MnTnHex-2-PyP^{5+} groups had 14 normal, 2 mild, 3 severely affected P1 kits (32 days of gestation) and 0 stillbirths, compared to saline with 4 normal, 3 mild, 5 severe, and 6 stillbirths from 2 dams/group. The enhanced ability to cross blood brain barrier contributed to the increased efficacy of MnTnHex-2-PyP^{5+} to prevent chronic morphine tolerance (anti-inflammatory condition) in a mouse pain model given intraperitoneally at 0.1 mg/kg/day for 4 days as compared to 3 mg/kg of MnTE-2-PyP^{5+} (Batinic-Haberle et al. 2009b). In a G93A mouse mutant amyotrophic lateral sclerosis study, three metalloporphyrins were thus far tested, FeTBAP^{3-}, MnTDE-2-ImP^{5+}, and MnTnHex-2-PyP^{5+}; the lipophilic MnTnHex-2-PyP^{5+} was efficacious at 5–10-fold lower dose than MnTDE-2-ImP^{5+} (Crow 2005, 2006; Crow et al. 2005). In a rat pulmonary radioprotection study, again, hexyl was more efficacious than ethyl porphyrin. In a radioprotection of ataxia telangiectasia (AT), among six Mn porphyrins, three Mn salens and two Mn cyclic polyamines tested, only a very lipophilic and cationic compound that possesses high antioxidant capacity, MnTnHex-2-PyP^{5+}, was protective (Pollard et al. 2009). Equally potent, but 13,500 more hydrophilic MnTE-2-PyP^{5+} was ineffective. Potent and lipophilic SOD mimic, Mn(II) cyclic polyamine lacks positive charges which likely

prevents its mitochondrial accumulation and therefore presumably its efficacy. Thus, the data indicate that mitochondrial accumulation, driven by positive charges and the lipophilicity of the compound, may play a critical role in AT model. Another support for the impact of mitochondrial accumulation on the in vivo efficacy of MnPs was provided from (1) our ongoing *Saccharomyces cerevisiae* studies where MnTnHex-2-PyP^{5+} when compared to MnTE-2-PyP^{5+} accumulates in mitochondria at significantly higher levels than in cytosol (Gralla et al., unpublished) as well as from (2) our mouse study where hexyl analog accumulates more in heart mitochondria than does ethyl porphyrin (Spasojevic et al. 2006, unpublished). The mouse ongoing MRI experiments at 7T show that following a single mouse injection, the relaxation changes of MnTnHex-2-PyP^{5+} in prostate tumors measure 10–11-fold greater than in normal prostate gland (Lascola et al. 2010).

The effect of the position of alkyl chains on meso pyridyl substituents—In the aerobic growth of SOD-deficient *E. coli*, the effect of the *ortho* versus *meta* position on *meso* pyridyls was established (Fig. 4); the tenfold increased lipophilicity of the *meta* isomer, MnTE-3-PyP^{5+}, with respect to the *ortho* analog MnTE-2-PyP^{5+} (Table 1) leads to its tenfold higher accumulation within *E. coli* which in turn fully compensates for the tenfold lower k_{cat} of the *meta* isomer. Consequently, *meta* isomer was equally efficient as *ortho* in rescuing SOD-deficient *E. coli* when it grew aerobically (Kos et al. 2009a).

Toxicity: The TD_{50} (the dose at which toxic effects were observed with 50% of mice) of MnTnHex-2-PyP^{5+} is 12.5 mg/kg when given subcutaneously (Pollard et al. 2009). Given its significantly increased efficacy, the therapeutic window, i.e. the ratio of toxic (12.5 mg/kg) to effective dose (0.4–0.05 mg/kg), is 31–250 for MnTnHex-2-PyP^{5+}, while it is 15 for MnTE-2-PyP^{5+} (91.5 mg/kg over 6 mg/kg) (Batinic-Haberle et al. 2010).

The impact of MnPs on cellular redox-based transcriptional activity

The decrease in oxidative stress injuries via scavenging ROS/RNS by Mn porphyrins have been shown in numerous studies, some reviewed in Batinic-Haberle et al. (2010). Among them are: (1) superoxide-specific effects exerted in *E. coli* study where SOD deficient *E. coli* grew aerobically only if medium was substituted for the cytoplasmic SOD enzymes; (2) radioprotective effects where MnP decreased oxidative damage by scavenging ROS/RNS; (3) ischemia/reperfusion injuries which involve burst in ROS/RNS upon reperfusion, etc. Yet, if a single dose of Mn porphyrins was given only at the moment of primary oxidative stress or prior to injury, the short-term protective effects were observed, but protection was not sustained over a long period of time (Sheng et al. 2009). Another interesting observation was recently made in a radioprotection (Gauter-Fleckenstein et al. 2010) and stroke study (Sheng et al. 2009): if the MnP was absent at the moment of primary oxidative stress but was given hours or weeks after it, the remarkable protective effects could still be achieved. Such observations indicate that Mn porphyrins are not merely scavenging ROS/RNS produced at the moment of initial oxidative insult. Several years ago two independent, diabetes and radiation/cancer, studies were the first to offer an explanation (Moeller et al. 2004; Piganelli et al. 2002; Bottino et al. 2004; Tse et al. 2004). In a diabetes-related study, MnTDE-2-ImP^{5+} prevented NF-κB activation (Tse et al. 2004; Bottino et al. 2004) and impacted NF-κB-dependent gene transcription. MnTDE-2-ImP^{5+} suppressed pro-inflammatory cytokine production and secondary inflammation as a result of oxidative stress and the ensuing cyclic inflammatory immune responses (Fig. 5). Radiation/cancer-related study on a 4T1 breast mouse carcinoma model (Moeller et al. 2004) assessed the effects of MnTE-2-PyP^{5+} on HIF-1α. Soon afterward, additional studies on a murine skin carcinogenesis model demonstrated that MnTE-2-PyP^{5+} inhibited AP-1 transcriptional activity (Zhao et al. 2005). Suppression of HIF-1α, VEGF, and TGF-β in rodent pulmonary radioprotection studies and LPS-stimulated macrophages were also shown (Gauter-

Fleckenstein et al. 2008, 2010). Below is the summary of the effects observed along with related mechanistic considerations in particular with respect to NF-κB. The data indicate that the inhibition of HIF-1α and AP-1 via antioxidant action likely occurs in the cytosol, while the impact upon NF-κB via pro-oxidative action seems to happen predominantly in nucleus.

HIF-1α—HIF-1α is a pro-angiogenic transcription factor that is activated under conditions of intermittent hypoxia and upregulates a number of genes including VEGF, EGF, and TGF-β to drive angiogenesis and fibrinogenesis. Recent studies have indicated how critical NF-κB signaling is to inflammatory gene expression and to the regulation of HIF-1α (Oliver et al. 2009). The very first data published on the inhibitory effect of MnTE-2-PyP^{5+} on HIF-1α activation in 4T1 mouse breast cancer cells that were exposed to H_2O_2 and $^{\bullet}NO$ (Fig. 5) (Moeller et al. 2004) were subsequently confirmed in a mouse breast cancer study where treatment of mice bearing 4T1 cells led to a significant inhibition of hypoxia, HIF-1α, VEGF, vascular density, and suppressed tumor growth (Rabbani et al. 2009). Importantly, oxidative stress, assessed through measuring 8-OHdG, nitrotyrosine, NADPH oxidase, and macrophages infiltration, was significantly reduced, leading to a conclusion that anti-angiogenic effects presumably arise from the decreased levels of ROS/RNS which in turn prevents activation of HIF-1α and expression of its downstream product, VEGF (Rabbani et al. 2009). Further support also comes from another recent study with *N*-acetylcysteine presumably suppressing tumor growth through inhibition of HIF-1α activation (Gao et al. 2007).

The effect of MnP on HIF-1α and VEGF was also observed in a radiosensitization study where MnTE-2-PyP^{5+} was administered immediately after each of three doses of 5 Gy radiation, separated by 12 h. Tumor vasculature density was decreased by 79% at 48 and 72 h after radiation, and tumor growth significantly suppressed; amifostine produced no effect (Moeller et al. 2005). In a parallel in vitro experiment, tumor cells were grown under hypoxic conditions (0.5% O_2), whereby releasing cytokines into medium (Moeller et al. 2005). If the growing medium, which lacked MnTE-2-PyP^{5+}, was collected and later used to grow endothelial cells for 2 h before radiation, the endothelial cells were fully viable as compared to the irradiated cells being in medium which was collected from tumor cells growing under hypoxic conditions with MnP added. MnTE-2-PyP^{5+} inhibited the release of cytokines (VEGF, EGF, etc.) from hypoxic tumor cells, which would have otherwise protected endothelial cells from irradiation.

In the same radiosensitization study (Moeller et al. 2005), no cytotoxicity of MnP to tumor cells (4T1 and R3232) was observed. Further, four different tumor cell lines, Hela cells, CaCo-2 cells, 4T1, and HCT116, were grown with MnTE-2-PyP^{5+} and MnTnHex-2-PyP^{5+} (Ye et al. 2009). No toxicity was observed with 10,000 cells/well at 30 μM MnP (Ye et al. 2009). At a higher cellular density of 50,000 cells/well, up to 1 mM both Mn porphyrin solutions were not cytotoxic.

In an in vitro study, alveolar macrophages under hypoxic conditions (0.5% of O_2) upregulated TGF-β and VEGF production, while MnTE-2-PyP^{5+} reduced their levels to basal (normoxic) values. Production of superoxide was also greatly enhanced under hypoxic conditions and normalized in the presence of MnTE-2-PyP^{5+} indicating the involvement of ROS and their scavengers in modulation of the cytokine expression (Jackson et al. 2007).

In rodent pulmonary radioprotection studies, Mn(III) *N*-alkylpyridyl- and *N*,*N*′-dialkylimidazolylporphyrins were effective when given before, immediately after injury, and even days or weeks after injury (Vujaskovic et al. 2002; Rabbani et al. 2007a, b). The protective effect was at the level of primary radiation injury and/or secondary oxidative events. In the most recent studies, histopathological and functional lung damage was

dramatically improved when 6 mg/kg/day MnTE-2-PyP^{5+} and 0.05–1 mg/kg/day MnTnHex-2-PyP^{5+} were given for 2 weeks started at different time points after the irradiation (Gauter-Fleckenstein et al. 2008, 2010). HIF-1α, VEGF, macrophage accumulation, oxidative stress (8-OHdG), TGF-β, and hypoxia were greatly reduced by the treatment. In a study with MnTE-2-PyP^{5+}, we have shown for the first time that it is able to reverse the overall rat lung damage even when its 2-week delivery started at the time of established lung injury, 8 weeks after the irradiation (Gauter-Fleckenstein et al. 2010).

AP-1—AP-1 transcription factor regulates gene expression and controls a number of cellular processes such as cell survival, proliferation, and death (Shaulian and Karin 2001). At the same time the inhibitory effect of MnP on HIF-1α was reported, the effects upon AP-1 in skin carcinogenesis were also noted (Zhao et al. 2005). Tumor was induced by the mutagenic initiator 7,12-dimethylbenz(α)-anthracene (DMBA) and promoted by 12-*O*-tetra-decanoylphorbol-13-acetate (TPA). MnTE-2-PyP^{5+} was applied to skin (5 ng/mouse/day) either at 30 min prior to TPA (MnP/TPA) or at 12 h following TPA application (TPA/MnP) 5 days/week for 14 weeks. The suppressive effect was much more significant when MnTE-2-PyP^{5+} was given 12 h following TPA treatment as cells undergo apoptosis but prior to proliferation. The decrease in oxidative stress by MnP paralleled AP-1 inhibition (Fig. 5). MnTE-2-PyP^{5+} further suppressed PCNA (proliferating cellular nuclear antigen, a well-recognized proliferative marker) and mitosis but not apoptosis, because it was given 12 h after TPA treatment as cells underwent apoptosis. The effect of MnTE-2-PyP^{5+} on tumor incidence and multiplicity was much greater with timed administration of SOD mimic than with MnSOD-overexpressed mice (where timely administration is impossible). Near full suppression of papillomas with MnTE-2-PyP^{5+} (31 vs. 5 in control group) as compared to 31 versus 17 in MnSOD-overexpressed mice was found. In a latter case, MnSOD affected both cell proliferation and apoptosis which diminished the final outcome (Zhao et al. 2001).

NF-kB—NF-κB family of transcription factors [p65 (RelA), RelB, c-Rel, NF-κB1 (p50 and its precursor p105), and NF-κB2 (p52 and its precursor p100)] controls hundreds of genes involved in regulation of immunity, development, apoptosis, cell proliferation, and inflammation (Gloire and Piette 2009; Oliveira-Marques et al. 2009). Its misregulation in cells is linked with several diseases including cancer, autoimmunity, and chronic inflammation. Therapies that specifically target this signaling pathway may prove to be efficacious in the treatment of various pro-inflammatory-mediated diseases since NF-κB activation is prevalent in arthritis, gastritis, inflammatory bowel disease, and sepsis. In resting cells, NF-κB proteins are sequestered in cytoplasm through their tight association with IκB proteins. The inhibition of NF-κB by MnP was first shown by the Piganelli group with nuclear extracts from LPS-treated bone marrow-derived macrophages (Tse et al. 2004; Bottino et al. 2004). Treatment with MnTE-2-PyP^{5+} and MnTDE-2-ImP^{5+} prevented the binding of the p50 subunit of the canonical NF-κB moiety to the cognate DNA response element. This inhibition of NF-κB DNA-binding abrogated the initiation of the innate immune response as evidenced by suppression of pro-inflammatory cytokine TNF-α and IL-1β. The authors showed that all other facets of NF-κB pathways were unaffected: IKKα/β phosphorylation, IκB-α phosphorylation/degradation, and NF-κB p50/p60 nuclear translocation. Furthermore, these results were recapitulated in human pancreatic islets under normal conditions and when pancreatic cells were cultured for 30 min with medium containing proteolytic enzymes and byproducts generated by pancreatic cells during isolation (Bottino et al. 2004). In the presence of 34 μM MnTDE-2-ImP^{5+}, a reduction in NF-κB-dependent gene transcription of cytokines and chemokines, such as IL-6, IL-8, and MCP-1 (macrophage chemoattractant porphyrin-1), was observed in addition to PARP [poly(ADP-ribose)polymerase] suppression.

The reducing environment in the nucleus is critical for NF-κB binding (Toledano et al. 1993; Gloire and Piette 2009) (Fig. 6). There are seven cysteine amino acids in NF-κB p50, and cysteine 62 is in a well-conserved Rel homology domain, characteristic of NF-κB family members and necessary for DNA-binding (Toledano et al. 1993). Point mutations of all seven cysteine amino acids in NF-κB p50 to serine did not abolish DNA-binding, but DNA-binding was prevented when cysteine 62 was oxidized with diamide or *N*-ethylmaleimide except for the C62S point mutant (Toledano et al. 1993). Therefore, cysteine 62 is the only amino acid that is redox-sensitive in NF-κB p50 (Toledano et al. 1993; Nishi et al. 2002; Matthews et al. 1992). In order to efficiently bind DNA, cysteine 62 of the NF-κB p50 subunit must be reduced. Had MnP exhibited antioxidative activity in the nucleus and further enhanced the reducing environment, NF-κB DNA binding would not have been suppressed. Therefore, the pro-oxidative action of MnPs has been proposed. Several quinones were reported to act similar to MnP in a pro-oxidative fashion (Gloire and Piette 2009). Quinones have been known to undergo one-electron reduction to semiquinone which in turn can be oxidized back to quinone, whereby reducing oxygen to superoxide (alike the ubiquinone in mitochondrial respiration). Several enzymes have been reported to control the redox state of cysteine 62 in NF-κB p50: thioredoxin (TRX) (Matthews et al. 1992) and AP endonuclease 1/redox factor 1 (APE1/Ref-1) (Jeon and Irani 2009), the latter acting either as a redox cofactor or redox chaperone (Fig. 6). Glutatione (GSH) is also transported into nucleus in early phases of cell growth when most of cells are in active division phase to assure reducing conditions (Markovic et al. 2007). GSH may directly act as a transcriptional regulator of NF-κB, AP-1, and p53 by altering nuclear redox state (Jang and Surh 2003). *S*-nitrosation of cysteines (Matthews et al. 1996) or nitration of tyrosines would also unfavor DNA binding (Fig. 6) (Gloire and Piette 2009). Taken together, our data suggest that MnP either directly oxidizes cysteine 62 of NF-kB p50, or prevents AEP1/Ref-1 and/or thioredoxin to secure the reduction of cysteine 62 and facilitate DNA binding (Gloire and Piette 2009).

$Mn^{III}P$ can oxidize glutathione (pK_a = 9.2) (Halliwell and Gutteridge 2007) as depicted in Fig. 7. The reaction is pH dependent, and is slow at pH 7.8 where the protonated thiol is a major species. At higher pH (≥9), where there is a significant contribution of reactive thiolate in solution, a reaction is much faster. The average pK_a of protein cysteine thiols is ~8.5. However, many proteins have domains that lower the pK_a significantly, so that under physiological conditions thiolate anion is a reactive species (Hill et al. 2009). Under such conditions (which would resemble the oxidation of GSH at higher pH; Fig. 7, spectrum 3), $Mn^{III}P$ would readily oxidize cysteines in vivo; $Mn^{III}P/Mn^{II}P$ redox couple would be employed. Further, under in vivo oxidative stress with increased levels of peroxide and/or peroxynitrite, $Mn^{III}P$ would likely be oxidized to some extent to a strongly oxidizing high-valent species $O=Mn^{IV}P$. We reported that $O=Mn^{IV}P$ rapidly oxidizes GSH (Ferrer-Sueta et al. 1999), and could thus efficiently oxidize cysteine 62; in such case $O=Mn^{IV}P/Mn^{III}P$ redox couple would be utilized.

A study (depicted in Fig. 8a) aimed to distinguish the effect of charges and the redox properties of Mn porphyrins and compounds of similar action on the inhibition of p50 DNA binding. The study was performed in a cell-free system where the likely scenario is the reduction of $Mn^{III}P$ to $Mn^{II}P$ with cysteine. In such a system the presence of ROS/RNS to promote the formation of $O–Mn^{IV}P$ and its consequent reduction to $Mn^{III}P$ with cysteine is unlikely. As noted above, the thiolate is presumably the reactive species of p50 cysteine (Hill et al. 2009). Thus, the positive charges on the porphyrins would favor the approach, and thus, the oxidation of cysteine, while the negatively charged compounds would be repelled from p50. Consequently, the proper electrostatics for the approach of the MnP to p50 protein and a proper reduction potential $E_{1/2}$ for $Mn^{III}P/Mn^{II}P$ redox couple are critical. The data in Fig. 8a clearly showed that compounds that are anionic or neutral at the

periphery ($MnTBAP^{3-}$, $MnhematoP^{-}$, $Mn(salen)^{+}$—EUK-8 and $MnCl_2$) do not prevent NF-kB p50 DNA binding, while all cationic porphyrins are suppressive ($MnTM\text{-}3\text{-}PyP^{5+}$, $MnTnHex\text{-}2\text{-}PyP^{5+}$, $MnTE\text{-}2\text{-}PyP^{5+}$, $MnTnBu\text{-}2\text{-}PyP^{5+}$, and $MnTMOE\text{-}2\text{-}PyP^{5+}$) (Fig. 8a). Among anionic porphyrins, $MnTBAP^{3-}$ and $MnhematoP^{-}$, with very negative $E_{1/2}$ of ≤ −200 mV versus NHE, are very redox-inert (only a strong reductant, sodium dithionite can reduce $MnTBAP^{3-}$) (Batinic-Haberle et al., unpublished), while $MnT(2,6\text{-}Cl_2\text{-}3\text{-}SO_3P)P^{3-}$ has ~300 mV more positive potential (+88 mV vs. NHE) which allows for a marginal effect, despite its anionic charges (Table 1).

High positive oxidation potential of $MnCl_2$ (+850 mV vs. NHE) allows it to act as reductant only, thus preventing it to oxidize SH groups. Among cationic compounds, the *meta* isomer, $MnTM\text{-}3\text{-}PyP^{5+}$, that is tenfold less potent antioxidant than $MnTE\text{-}2\text{-}PyP^{5+}$ and has $E_{1/2}$ inferior to that of $MnT(2,6\text{-}Cl_2\text{-}3\text{-}SO_3P)P^{3-}$ (+52 mV vs. NHE), is still able to fully suppress p50 DNA binding. *Such data support the notion that electrostatics plays major role; however, the favorable thermodynamics could outbalance the unfavorable electrostatics to some extent.* The commercial $MnTBAP^{3-}$ used in this study had Mn oxo/hydroxo/acetato impurities that possess high SOD-like activity (Rebouças et al. 2008a, b, c). Those impurities are negatively charged at the periphery and did not inhibit NF-*κ*B p50 DNA binding. Further, $MnCl_2$ and $Mn(salen)^{+}$ that bear positive charge on a metal site only, are stabilized in their respective (+2 and +3) oxidation states. Yet, in vivo, in addition to the interaction of MnP with p50, the accumulation of MnP would play a major role. The anionic compounds may not enter nucleus to any significant degree. If the anionic charges allowed their nuclear localization, in an oxidizing environment, anionic compounds such as $MnTBAP^{3-}$ could be oxidized to a high-valent, oxidizing Mn(IV) species with either peroxide or peroxynitrite (Ferrer-Sueta et al. 2003), which in turn could oxidize cysteine SH groups to some extent despite the unfavorable electrostatics.

Additional experiments were designed to provide evidence that the cationic porphyrin, $MnTE\text{-}2\text{-}PyP^{5+}$, accumulates in the nucleus. Bone marrow-derived macrophages were stimulated with LPS and treated with 34 μM $MnTE\text{-}2\text{-}PyP^{5+}$ for 1.25 h. As expected, the accumulation of cationic $MnTE\text{-}2\text{-}PyP^{5+}$ in nucleus was threefold higher than in the cytosol (Fig. 8b). The cationic compounds appear to be attracted toward the nucleus by the negatively charged phosphate groups of nucleic acids.

Warner et al. have recently shown in a 90-min middle cerebral artery occlusion stroke model that suppression of NF-*κ*B activation mediated by $MnTDE\text{-}2\text{-}ImP^{5+}$ contributes in part to the improvement in neurologic and histologic outcome (including decrease in cortical and subcortical infarct volume) at 8 weeks after reperfusion, if the MnP was given intracerebroventricularly to rats for 1 week starting at 90 min after reperfusion (Sheng et al. 2009). This was demonstrated by NF-*κ*B electrophoretic mobility shift assay performed at 6 h after reperfusion (Fig. 5). In ischemic hemisphere the p50 NF-*κ*B subunit DNA binding was fully suppressed, but was not prevented in contralateral hemisphere. The same effect on NF-*κ*B and neurologic and histologic outcome has recently been observed with $MnTnHex\text{-}2\text{-}PyP^{5+}$ (Warner et al. 2010). However, due to the 13,500-fold increased lipophilicity and 12-fold increased distribution in brain versus plasma when compared to hydrophilic analogs such as $MnTE\text{-}2\text{-}PyP^{5+}$ (Doyle et al. 2009), $MnTnHex\text{-}2\text{-}PyP^{5+}$ provided remarkable protection when given iv; in addition, it has significantly smaller effect on decreasing blood pressure than $MnTE\text{-}2\text{-}PyP^{5+}$ and $MnTDE\text{-}2\text{-}ImP^{5+}$ (Warner et al. 2010).

It is still possible that interactions of porphyrins with p50 subunit other than pro-oxidative and possibly electrostatic in nature (based on porphyrin cationic character) are operative. Cationic MnP could compete with p50 binding to the negatively charged DNA binding sites.

As already noted, it is also possible that MnP could oxidize cysteines of Ref-1 or glutathione, rather than of p50 subunit. The use of redox-inactive metal-free ligand or Zn porphyrin to distinguish between redox and electrostatic effects has thus far proved difficult as those compounds are potent photosensitizers. The use of p50 C62S mutant (Matthews et al. 1992) that binds to DNA while not possessing a redox-sensitive cysteine p62 would perhaps provide additional evidences for the nature of events occurring in the nucleus.

Based on published reports, HIF-1α seems to be under the control of NF-κB via cyclooxygenase/prostaglandin (Bonello et al. 2007; Sun et al. 2007) and canonical signaling pathways [activated through the IκB kinase (IKK) complex consisting of IKKα, IKKβ, IKKγ, which usually results in nuclear localization of p65/p50 dimers] (Oliver et al. 2009). Thus, the effects of Mn porphyrins on HIF-1α may be at least in part influenced by the impact of MnP on NF-κB. Further studies would aim to distinguish between NF-κB and HIF-1α-based effects.

SP-1—This transcription factor plays multiple and sophisticated roles as a modulator of tissue-specific transcription. Activity of SP-1 shows complex regulation by glycosylation, phosphorylation, oxidative stress, proteolytic cleavage, and other transcription factors including NF-κB (Fountain et al. 2007). In a manner similar to NF-κB, MnTDE-2-ImP^{5+} was shown to inhibit SP-1 DNA binding (Tse et al. 2004). The ability of MnTM-2-PyP^{5+} to prevent the induction of the Na^+/H^+ exchangers NHE-1 and NHE-3 and to reduce the activity of the Na^+/K^+-ATPase in a rat diabetes model is presumably due to the interference of MnP with SP-1 activation (Khan et al. 2009). NHE together with ubiquitously expressed Na^+/K^+-ATPase maintains Na^+ and fluid homeostasis, the latter being also regulated by NF-κB and AP-1 transcription factors.

In summary, the inhibition of NF-κB activation in activated macrophages (Tse et al. 2004) was the very first example demonstrating that MnP could exert beneficial effects on cellular transcriptional activity via pro-oxidative action. As shown above, ROS/RNS activate transcription factors and their removal (presumably in cytosol) fully suppressed their activation (Fig. 5). Modulation of cellular and subcellular redox status by MnP compounds can affect gene transcription by either reducing or increasing levels of oxidants as dictated by the charge and subcellular compartmentalization of MnP compounds. Further studies are needed to elucidate if the pro-oxidative action of MnPs involved in suppressing NF-κB activation in nucleus may also be operative for other redox-sensitive transcription factors.

Cancer studies

Recently, it was shown that at least in part, MnTE-2-PyP^{5+} sensitized murine thymic lymphoma cells, WEHI7.2, to glucocorticoid and cyclophosphamide treatment, suppressing their growth via pro-oxidative action, presumably via H_2O_2 production (Jaramillo et al. 2009). Similarly, the Li et al. (2000) results (reviewed in Holley et al. 2010) on human glioma cells showed that GPX overexpression not only reversed the tumor cell growth inhibition caused by MnSOD overexpression, but also altered the cellular contents of total glutathione, reduced glutathione, oxidized glutathione, and intracellular reactive oxygen species. The results suggest that hydrogen peroxide or other hydroper-oxides appear to be key reactants in the tumor suppression by MnSOD overexpression and that growth inhibition correlates with the intracellular redox status.

As already noted and reported, Mn porphyrin with $E_{1/2}$ ~ +200 mV versus NHE can easily donate and accept electrons from redox able compounds, such as are cellular reductants. As stated above, cellular reductants readily reduce porphyrin to $Mn^{II}P$ (Batinic-Haberle et al. 2004), which in turn can react both with superoxide and oxygen. Though the reaction with

$O_2^{\bullet -}$ is much faster than with oxygen, the higher levels of oxygen may favor reaction of $Mn^{II}P$ with O_2. Binding of oxygen to Mn center would lead to cyt P450-like chemistry where highly oxidizing species H_2O_2 and $O{=}Mn^{IV}P$ would be formed (Spasojevic et al. 2006). Also, were the cellular reductants depleted and levels of H_2O_2 increased, the $O{=}Mn^{IV}P$ would be formed (from $Mn^{III}P$), and if not reduced back to $Mn^{III}P$ with cellular reductants, it would oxidize biological targets such as cysteines of signaling proteins (Ferrer-Sueta et al. 1999). We have performed the in vitro studies on four cancer cell lines in the presence of MnP and ascorbate alone and in their combination. When combined, H_2O_2 was produced. Tumor cell survival data from the clonogenic assay agree well with the tetrazolium salt WST-1 data (the latter assay assesses the metabolically active cells). The combination of ascorbate and MnP is highly cytotoxic to tumor cells; the cells were not able to establish colonies anymore (Ye et al. 2009).

Concluding remarks

When compared to other types of synthetic antioxidants, Mn porphyrins possess: (1) highest k_{cat} ($O_2^{\bullet -}$) and k_{red} ($ONOO^-$); (2) extreme metal/ligand stability to assure the integrity of the redox active Mn site, and (3) countless possibilities of derivatization to optimize the potency, bioavailability, and the toxicity. Though such properties make them advantageous over other types of synthetic antioxidants for treating diseases that have oxidative stress in common, comparative studies are still needed to fully assess the impact of different compounds in the same and different models of oxidative stress disorders.

Given the wealth of data, the present prevailing understanding is that potent catalytic antioxidants Mn(III) *N*-alkylpyridylporphyrins scavenge ROS/RNS ($O_2^{\bullet -}$, $ONOO^-$, $CO_3^{\bullet -}$, HClO and others) and decrease primary oxidative stress to biological molecules. By doing this, they eliminate the signal for upregulation of inflammatory-mediated pathways via suppression of redox-sensitive transcription factors (Fig. 9). The site of action is yet to be fully recognized, but is likely the cytosol.

Yet, the NF-κB data indicate that at least in part MnPs may provide beneficial effects through pro-oxidative action in the nucleus by oxidizing redox-sensitive transcription factors and thus preventing their DNA binding. Consequently, the excessive upregulation of inflammatory and immune responses is suppressed. Lymphoma cancer (Jaramillo et al. 2009) and our 4T1 mouse breast cancer studies (Ye et al. 2009) also demonstrate that at least in part the pro-oxidative action of MnPs may contribute to antitumorigenesis.

Finally, not to detail here, as this is the subject of other manuscript within the same issue (Benov et al. 2010), photodynamic therapy with redox-inactive, metal-free ligands and Zn porphyrins utilizes pro-oxidative action of porphyrins to inactivate critical proteins which in turn lead to cell killing (Al-Mutairi et al. 2007; Benov et al. 2010).

In addition to the above-mentioned actions of MnPs, Tauskela and Brunette (2009) have repeatedly suggested that action(s) other than antioxidative may be involved in neuroprotection, such as impact of porphyrins on Ca^{2+} metabolism. Their data on redox-active and redox-inactive compounds are not fully consistent (Tauskela et al. 2005), suggesting that the compounds might not have been sufficiently characterized with respect to identity and purity to fully support their conclusions. For example, the possibility that porphyrins interact with proteins through electrostatic and/or hydrophobic interactions and not via pro-oxidative action may not be fully excluded. Multiple actions of a single MnP are highly likely in vivo. Further studies would hopefully increase our insight into Mn porphyrins action/s in vivo.

It is important to point out that either for mechanistic studies or for development of MnPs as therapeutics their highest possible purity is of key importance. In several occasions thus far, the preparations that contained as little as ~20% of the MnTE-2-PyP^{5+} were used (Munroe et al. 2007; Warner et al., unpublished; Rebouças et al. 2008c). Also routinely, commercial preparations of MnTBAP^{3-} were used in published studies. We have shown that such MnTBAP^{3-} preparations not only differ among commercial sources, but also differ from batch to batch within one commercial source and may contain high levels of "free" Mn and photosensitizer, metal-free porphyrin (Rebouças et al. 2008a, b, c; Batinic-Haberle et al. 2009a, 2010).

All the data thus far published on MnPs are intriguing. Given the remarkable potential of metalloporphyrins as therapeutics, the elucidation of their role(s) in vivo is important and is of interest not only for clinicians, but for mechanistic studies as well.

Acknowledgments

In writing this review, we acknowledge the financial help from the National Institutes for Allergy and Infectious Diseases [U19AI067798]; Duke University's CTSA grant 1 UL 1 RR024128-01 from NCRR/NIH and NIH R01 DA024074; IS thanks NIH/NCI Duke Comprehensive Cancer Center Core Grant [5-P30-CA14236-29], and ZV to RO1 CA 098452. DKStC is grateful to CA 139843 and CA 07359. HMT is thankful to Cochrane-Weber Research Award and Research Advisory Council Award (Children's Hospital of Pittsburgh and the University of Pittsburgh), MWD to CA40355-25, and JDS to Juvenile Diabetes Association #1-2005-80, American Diabetes Association CDA 7-07 CD-16. The authors appreciate helpful discussions with Gerardo Ferrer-Sueta.

Abbreviations

ROS	Reactive oxygen species
RNS	Reactive nitrogen species
Peroxynitrite	$ONOO^- + H^+ \rightarrow ONOOH$ (pK_a= 6.6, at pH 7.8 peroxynitrite exists predominantly as $ONOO^-$)
$O_2^{\bullet -}$	Superoxide anion radical
$^{\bullet}$NO	Nitric oxide
$CO_3^{\bullet -}$	Carbonate anion radical
MnP	Mn porphyrin in +3 ($Mn^{III}P$) and +2 ($Mn^{II}P$) oxidation states; when porphyrins bear 5+ charge; they have Mn in +3 oxidation state; with 4+total charge, Mn is in +2 oxidation state, except in $O=Mn^{IV}P^{4+}$ where it is in +4 oxidation state
5, 10, 15, and 20	*meso* positions of the porphyrin ring (Fig. 2)
MnT-2(or 3 or 4)-PyP$^+$	Mn(III) *meso*-tetrakis[2(or 3 or 4)-pyridyl]porphyrin; 2, 3 and 4 relate to *ortho*, *meta* and *para* isomers, respectively (Fig. 2)
MnTPP$^+$	Mn(III) *meso*-tetraphenylporphyrin
MnTalkyl-2 (or 3 or 4)-PyP^{5+}	Mn(III) *meso*-tetrakis(*N*-alkylpyri-dinium-2(or 3 or 4)-yl)porphyrin, alkyl being methyl (M in *ortho*, *2* position, AEOL10112), ethyl (E in *ortho*, *2* position, AEOL10113, FBC-007), *n*-propyl (nPr), *n*-butyl (nBu), *n*-hexyl (nHex), *n*-heptyl (nHep), *n*-octyl (nOct)

MnBM-2-PyP^{5+}	5,10-bis(2-pyridyl)-15,20-bis (*N*-methylpyridinium-2-yl)porphyrin
MnTrM-2-PyP^{5+}	5-(2-pyridyl)-10,15,20-tris (*N*-methylpyridinium-2-yl)porphyrin
MnT(TFTMA)P^{5+}	5,10,15,20-tetrakis (2,3,5,6-tetrafluoro-*N*,*N*,*N*-trimethylanilinium-4-yl)porphyrin
MnBr$_8$TM-3-PyP^{4+}	Mn(II) *β*-octabromo-*meso*-tetrakis (*N*-methylpyridinium-3-yl) porphyrin
MnBr$_8$TM-4-PyP^{4+}	Mn(II) *β*-octabromo-*meso*-tetrakis (*N*-methylpyridinium-4-yl) porphyrin
MnCl$_{1\text{-}4}$TE-2-PyP^{5+}	Mn(III) *β*-(mono-tetra) chloro-*meso*-tetrakis (*N*-ethylpyridinium-2-yl)porphyrin
MnCl$_5$TE-2-PyP^{4+}	Mn(II) *β*-pentachloro-*meso*-tetrakis (*N*-ethylpyridinium-2-yl)porphyrin
MnTSPP^{3-}	Mn(III) *meso*-tetrakis (4-sulfonatophenyl)porphyrin
MnTBAP^{3-}	Mn(III) *meso*-tetrakis (4-carboxylatophenyl)porphyrin (also abbreviated as MnTCPP^{3-})
MnBr$_8$TSPP^{3-}	Mn(III) *β*-octabromo-*meso*-tetrakis (4-sulfonatophenyl)porphyrin
MnT(2,6-Cl$_2$-3-SO$_3$P)P^{3-}	Mn(III) *meso*-tetrakis (2,6-dichloro-3-sulfonatophenyl) porphyrin
MnhematoP^{-}	Mn(III) hematoporphyrin IX
FeTBAP^{3-}	Fe(III) *meso*-tetrakis (4-carboxylatophenyl)porphyrin (also abbreviated as FeTCPP^{3-})
MnTDE(M)-2-ImP^{5+}	Mn(III) *meso*-tetrakis[*N*,*N*′-diethyl (or dimethyl)imidazolium-2-yl) porphyrin; diethyl analog is AEOL10150
MnTMOE-2-PyP^{5+}	Mn(III) *meso*-tetrakis (*N*-methoxyethylpyridinium-2-yl)porphyrin
MnTDMOE-2-ImP^{5+}	Mn(III) *meso*-tetrakis[*N*,*N*′-di (2-methoxyethyl) imidazolium-2-yl]porphyrin
MnTM,MOE-2-ImP^{5+}	Mn(III) tetrakis [*N*-*methyl*-*N*′-methoxethyl) imidazolium-2-yl]porphyrin
Salen	*N*,*N*′-bis-(salicylideneamino) ethane
Mn(salen)$^{+}$	Known as EUK-8
$\boldsymbol{P_{OW}}$	Partition coefficient between *n*-octanol and water
TLC	Thin-layer chromatography
$\boldsymbol{R_f}$	Thin-layer chromatographic retention factor that presents the ratio between the compound and solvent path in 10:10:80 = sat. KNO_3(aq): H_2O:acetonitrile
$\boldsymbol{E_{1/2}}$	Half-wave reduction potential

SOD	Superoxide dismutase
NHE	Normal hydrogen electrode
HIF-1*α*	Hypoxia inducible factor-1*α*
NF-*κ*B	Nuclear factor *κ*B
AP-1	Activator protein-1
SP-1	Specificity protein-1
TF	Transcription factor
TPA	12-*O*-tetradecanoylphorbol-13-acetate
MCAO	Middle cerebral artery occlusion
NOS	Nitric oxide synthase
TRX	Thioredoxin
GSH	Glutathione
p^{65} and p^{50}	NF-*κ*B subunits

References

Al-Mutairi D, Craik JD, Batinic-Haberle I, Benov L. Inactivation of metabolic enzymes by photo-treatment with zinc *meta N*-methylpyridylporphyrin. Biochim Biophys Acta. 2007; 1770:1520–1527. [PubMed: 17884296]

Archibald FS, Fridovich I. The scavenging of superoxide radical by manganous complexes: in vitro. Arch Biochem Biophys. 1982; 214:452–463. [PubMed: 6284026]

Barnese K, Gralla EB, Cabelli DE, Valentine JS. Manganous phosphate acts as a superoxide dismutase. J Am Chem Soc. 2008; 130:4604–4606. [PubMed: 18341341]

Batinic-Haberle I, Benov L, Spasojević I, Fridovich I. The *ortho* effect makes manganese (III) *meso*-tetrakis(*N*-methylpy-ridinium-2-yl)porphyrin (MnTM-2-PyP) a powerful and potentially useful superoxide dismutase mimic. J Biol Chem. 1998; 273:24521–24528. [PubMed: 9733746]

Batinic-Haberle I, Benov L, Spasojević I, Hambright P, Crumbliss AL, Fridovich I. The relationship between redox potentials, proton dissociation constants of pyrrolic nitrogens, and in vitro and in vivo superoxide dismutase activities of manganese(III) and iron(III) cationic and anionic porphyrins. Inorg Chem. 1999; 38:4011–4022.

Batinic-Haberle I, Spasojević I, Stevens RD, Hambright P, Fridovich I. Manganese(III) *meso* tetrakis *ortho N*-alkylpyridylporphyrins. Synthesis, characterization and catalysis of O2•− dismutation. J Chem Soc Dalton Trans. 2002:2689–2696.

Batinic-Haberle I, Spasojević I, Stevens RD, Hambright P, Neta P, Okado-Matsumoto A, Fridovich I. New class of potent catalysts of O2•− dismutation. Mn(III) methoxyethylpyridyl- and methoxyethylimidazolylporphyrins. Dalton Trans. 2004:1696–1702. [PubMed: 15252564]

Batinic-Haberle I, Spasojevic I, Stevens RD, Bondurant B, Okado-Matsumoto A, Fridovich I, Vujaskovic Z, Dewhirst MW. New PEG-ylated Mn(III) porphyrins approaching catalytic activity of SOD enzyme. Dalton Trans. 2006:617–624. [PubMed: 16402149]

Batinic-Haberle I, Cuzzocrea S, Rebouças JS, Ferrer-Sueta G, Mazzon E, Di Paola R, Radi R, Spasojević I, Benov L, Salvemini D. Pure MnTBAP selectively scavenges peroxynitrite over superoxide: comparison of pure and commercial MnTBAP samples to MnTE-2-PyP in two different models of oxidative stress injuries, SOD-specific *E. coli* model and carrageenan-induced pleurisy. Free Radic Biol Med. 2009a; 46:192–201. [PubMed: 19007878]

Batinic-Haberle I, Ndengele MM, Cuzzocrea S, Rebouças JS, Masini E, Spasojević I, Salvemini D. Lipophilicity is a critical parameter that dominates the efficacy of metalloporphyrins in blocking

morphine tolerance through peroxynitrite-mediated pathways. Free Radic Biol Med. 2009b; 46:212–219. [PubMed: 18983908]

Batinic-Haberle I, Reboucas J, Spasojevic I. Superoxide dismutase mimics: chemistry, pharmacology and therapeutic potential. Antioxid Redox Signal. 201010.1089/ars.2009.2876

Benov L, Craik J, Batinic-Haberle I. Protein damage by photoactivated Zn(II) *N*-alkylpyridylporphyrins. Amino Acids. 2010 in press.

Bonello S, Zahringer C, BelAiba RS, Djordjevic T, Hess J, Michiels C, Kietzmann T, Gorlach A. Reactive oxygen species activate the HIF-1 promoter via a functional NF-κB. Arterioscler Thromb Vasc Biol. 2007; 27:755–761. [PubMed: 17272744]

Bottino R, Balamurugan AN, Tse H, Thirunavukkarasu C, Ge X, Profozich J, Milton M, Ziegenfuss A, Trucco M, Piganelli JD. Response of human islets to isolation stress and the effect of antioxidant treatment. Diabetes. 2004; 53:2559–2568. [PubMed: 15448084]

Carnieri N, Harriman A, Porter G. Photochemistry of manganese porphyrins. Part 6. Oxidation-reduction equilibria of manganese(III) porphyrins in aqueous solution. J Chem Soc Dalton Trans. 1982:931–938.

Crow, JP. Administration of Mn porphyrin and Mn texaphyrin at symptom onset extends survival of ALS mice. Doctrow, SR.; McMurry, TJ.; Sessler, SJ., editors. Vol. 903. American Chemical Society; Washington, DC: 2005. p. 295-318.

Crow J. Catalytic antioxidants to treat amyotrophic lateral sclerosis. Expert Opin Invest Drugs. 2006; 15:1383–1392.

Crow JP, Calinasan NY, Chen J, Hill JL, Beal MF. Manganese porphyrin given at symptom onset markedly extends survival of ALS mice. Ann Neurol. 2005; 58:258–265. [PubMed: 16049935]

DeFreitas-Silva G, Rebouças JS, Spasojević I, Benov L, Idemori YM, Batinic-Haberle I. SOD-like activity of Mn(II) β-octab-romo-meso-tetrakis(*N*-methylpyridinium-3-yl)porphyrin equals that of the enzyme itself. Arch Biochem Biophys. 2008; 477:105–112. [PubMed: 18477465]

Doyle T, Bryant L, Batinic-Haberle I, Little J, Cuzzocrea S, Masini E, Spasojevic I, Salvemini D. Supraspinal inactivation of mitochondrial superoxide dismutase is a source of peroxynitrite in the development of morphine antinociceptive tolerance. Neuroscience. 2009; 164:702–710. [PubMed: 19607887]

Faulkner KM, Liochev SI, Fridovich I. Stable Mn(III) porphyrins mimic superoxide dismutase in vitro and substitute for it in vivo. J Biol Chem. 1994; 269:23471–23476. [PubMed: 8089112]

Ferrer-Sueta G, Radi R. Chemical biology of peroxynitrite: kinetics, diffusion, and radicals. ACS Chem Biol. 2009; 4:161–177. [PubMed: 19267456]

Ferrer-Sueta G, Batinic-Haberle I, Spasojević I, Fridovich I, Radi R. Catalytic scavenging of peroxynitrite by isomeric Mn(III) *N*-methylpyridylporphyrins in the presence of reductants. Chem Res Toxicol. 1999; 12:442–449. [PubMed: 10328755]

Ferrer-Sueta G, Vitturi D, Batinic-Haberle I, Fridovich I, Goldstein S, Czapski G, Radi R. Reactions of manganese porphyrins with peroxynitrite and carbonate radical anion. J Biol Chem. 2003; 278:27432–27438. [PubMed: 12700236]

Ferrer-Sueta G, Hannibal L, Batinic-Haberle I, Radi R. Reduction of manganese porphyrins by flavoenzymes and submitochondrial particles and the catalytic redox cycle of peroxynitrite. Free Radic Biol Med. 2006; 41:503–512. [PubMed: 16843831]

Fountain SJ, Cheong A, Li J, Dondas NY, Zeng F, Wood IC, Beech DJ. $K_V1.5$ potassium channel gene regulation by Sp1 transcription factor and oxidative stress. Am J Physiol Heart Circ Physiol. 2007; 293:H2719–H2725. [PubMed: 17660393]

Gao P, Zhang H, Dinavahi R, Li F, Xiang Y, Raman V, Bhujwalla ZM, Felsher DW, Cheng L, Pevsner J, Lee LA, Semenza GL, Dang CV. HIF-dependent antitumorigenic effect of antioxidants in vivo. Cancer Cell. 2007; 12:230–238. [PubMed: 17785204]

Gauter-Fleckenstein B, Fleckenstein K, Owzar K, Jiang C, Batinic-Haberle I, Vujasković Z. Comparison of two Mn porphyrin-based mimics of superoxide-dismutase (SOD) in pulmonary radioprotection. Free Radic Biol Med. 2008; 44:982–989. [PubMed: 18082148]

Gauter-Fleckenstein B, Fleckenstein K, Owzar K, Jiang C, Rebouças JS, Batinic-Haberle I, Vujasković Z. Early and late administration of antioxidant mimic MnTE-2-PyP^{5+} in mitigation and treatment

of radiation-induced lung damage. Free Radic Biol Med. 2010; 48:1034–1043. [PubMed: 20096348]

Gloire G, Piette J. Redox regulation of nuclear post-translational; modifications during NF-κB activation. Antioxid Redox Signal. 2009; 11:2209–2222. [PubMed: 19203223]

Goldstein S, Fridovich I, Czapski G. Kinetic properties of Cu, Zn-superoxide dismutase as a function of metal content: Order restored. Free Radic Biol Med. 2006; 41:937–941. [PubMed: 16934676]

Halliwell, B.; Gutteridge, JMC. Free radical biology and medicine. 4. Oxford University Press; Oxford: 2007.

Hill BG, Reily C, Oh J-Y, Johnson MS, Landar A. Methods for the determination and quantification of the reactive thiol proteome. Free Radic Biol Med. 2009; 47:675–683. [PubMed: 19527783]

Holley AK, Dhar SK, Xu Y, StClair DK. Manganese superoxide dismutase: beyond life and death. Amino Acids. 2010 in press.

Jackson IL, Chen L, Batinic-Haberle I, Vujasković Z. Superoxide dismutase mimetic reduces hypoxia-induced O2•−, TGF-*β*, and VEGF production by macrophages. Free Radic Res. 2007; 41:8–14. [PubMed: 17164174]

Jang JH, Surh YJ. Potentiation of cellular antioxidant capacity by Bcl-2: implications for its antiapoptotic function. Biochem Pharmacol. 2003; 66:1371–1379. [PubMed: 14555211]

Jaramillo MC, Frye JB, Crapo JD, Briehl MM, Tome ME. Increased manganese superoxide dismutase expression or treatment with manganese porphyrin potentiates dexamethasone-induced apoptosis in lymphoma cells. Cancer Res. 2009; 69:5450–5457. [PubMed: 19549914]

Jeon H, Irani K. APE/REF-1: versatility in progress. Antioxid Redox Signal. 2009; 11:571–573. [PubMed: 18715142]

Jones DP. Radical-free biology of oxidative stress. Am J Physiol Cell Physiol. 2008; 295:C849–C868. [PubMed: 18684987]

Kachadourian R, Batinic-Haberle I, Fridovich I. Mn(III)Cl4T-2-PyP5+ exhibits a high superoxide dismuting rate. Free Radic Biol Med. 1998; 25:S17.

Kachadourian R, Johnson CA, Min E, Spasojević I, Day BJ. Flavin-dependent antioxidant properties of a new series of *meso*N,*N*′-dialkyl-imidazolium substituted manganese(III) porphyrins. Biochem Pharmacol. 2004; 67:77–85. [PubMed: 14667930]

Khan I, Batinic-Haberle I, Benov L. Effect of potent redox-modulating manganese porphyrin, MnTM-2-PyP, on the Na^+/H^+ exchangers NHE-1 and NHE-3 in the diabetic rat. Redox Rep. 2009; 14:236–242. [PubMed: 20003708]

Klug-Roth D, Fridovich I, Rabbani J. Pulse radiolytic investigations of superoxide catalyzed disproportionation. Mechanism for bovine superoxide dismutase. J Am Chem Soc. 1973; 95:2786–2790. [PubMed: 4632912]

Koner R, Goldberg I. Crystal engineering of molecular networks. Hydrogen bonding driven two-dimensional assemblies of tetrapyridylporphyrin with benzene tri- and tetra-carboxylic acids. CrystEngComm. 2009; 11:1217–1219.

Kos I, Benov L, Spasojević I, Rebouças JS, Batinic-Haberle I. High lipophilicity of *meta* Mn(III) *N*-alkylpyridylporphyrin-based SOD mimics compensates for their lower antioxidant potency and makes them equally effective as *ortho* analogues in protecting *E. coli*. J Med Chem. 2009a; 52:7868–7872. [PubMed: 19954250]

Kos I, Rebouças JS, DeFreitas-Silva G, Salvemini D, Vujasković Z, Dewhirst MW, Spasojević I, Batinic-Haberle I. The effect of lipophilicity of porphyrin-based antioxidants. Comparison of *ortho* and *meta* isomers of Mn(III) *N*-alkylpyridylporphyrins. Free Radic Biol Med. 2009b; 47:72–78. [PubMed: 19361553]

Lascola, CD.; Batinic-Haberle, I.; Talaignar, V.; Amrhein, T.; Mouraviev, V.; Wang, H. Mn-porphyrin SOD mimetics as novel NMR imaging probes. 6th international conference on porphyrins and phthalocyanines; New Mexico. 2010.

Lee J, Hunt JA, Groves JT. Manganese porphyrins as redox-coupled peroxynitrite reductases. J Am Chem Soc. 1998; 120:6053–6061.

Li S, Yan T, Yang J-Q, Oberley TD, Oberley LW. The role of cellular glutathione peroxidase redox regulation in the suppression of tumor cell growth by manganese superoxide dismutase. Cancer Res. 2000; 60:3927–3939. [PubMed: 10919671]

Mackensen GB, Patel M, Sheng H, Calvi CL, Batinic-Haberle I, Day BJ, Liang LP, Fridovich I, Crapo JD, Pearlstein RD, Warner DS. Neuroprotection from delayed post-ischemic administration of a metalloporphyrin catalytic antioxidant in the rat. J Neurosci. 2001; 21:4582–4592. [PubMed: 11425886]

Markovic J, Borras C, Ortega A, Sastre J, Vina J, Pallardo FV. Glutathione is recruited into nucleus in early phases of cell proliferation. J Biol Chem. 2007; 282:20416–20424. [PubMed: 17452333]

Matthews JR, Wakasugi N, Virelizier J-L, Yodoi J, Hay RT. Thioredoxin regulates the DNA binding activity of NF-κB by reduction of a disulphide bond involving cysteine 62. Nucleic Acid Res. 1992; 20:3821–3830. [PubMed: 1508666]

Matthews JR, Botting CH, Panico M, Morris HR, Hay RT. Inhibition of NF-κB DNA binding by nitric oxide. Nucleic Acid Res. 1996; 24:2236–2242. [PubMed: 8710491]

McCord JM. The evolution of free radicals and oxidative stress. Am J Med. 2000; 108:652–659. [PubMed: 10856414]

McCord JM. Superoxide dismutase, lipid peroxidation, and bell-shaped dose response curves. Dose Response. 2008; 6:223–228. [PubMed: 18846257]

Michel E, Nauser T, Sutter B, Bounds PL, Koppenol WH. Kinetics properties of Cu, Zn-superoxide dismutase as a function of metal content. Arch Biochem Biophys. 2005; 439:234–240. [PubMed: 15978540]

Moeller BJ, Cao Y, Li CY, Dewhirst MW. Radiation activates HIF-1 to regulate vascular radiosensitivity in tumors: role of oxygenation, free radicals and stress granules. Cancer Cell. 2004; 5:429–441. [PubMed: 15144951]

Moeller BJ, Batinic-Haberle I, Spasojević I, Rabbani ZN, Anscher MS, Vujasković Z, Dewhirst MW. A manganese porphyrin superoxide dismutase mimetic enhances tumor radioresponsiveness. Int J Rad Oncol Biol Phys. 2005; 63:545–552.

Munroe W, Kingsley C, Durazo A, Gralla EB, Imlay JA, Srinivasan C, Valentine JS. Only one of a wide assortment of manganese-containing SOD mimicking compounds rescues the slow aerobic growth phenotype of both *Escherichia coli* and *Saccharomyces cerevisiae* strains lacking superoxide dismutase enzymes. J Inorg Biochem. 2007; 101:1875–1882. [PubMed: 17723242]

Murphy MP. Targeting lipophilic cations to mitochondria. Biochim Biophys Acta. 2008; 177:1028–1031. [PubMed: 18439417]

Nishi T, Shimizu N, Hiramoto M, Sato I, Yamaguchi Y, Hasegawa M, Aizawa S, Tanaka H, Kataoka K, Watanabe H, Handa H. Spatial redox regulation of a critical cysteine residue of NF-κB in vivo. J Biol Chem. 2002; 277:44548–44556. [PubMed: 12213807]

Oliveira-Marques V, Marinho S, Cyrne L, Antunes F. Role of hydrogen peroxide in NF-κB activation: From inducer to modulator. Antioxid Redox Signal. 2009; 11:2223–2243. [PubMed: 19496701]

Oliver KM, Garvey JF, Teck Ng C, Veale DJ, Fearon U, Cummins EP, Taylor CT. Hypoxia activates NF-κB-dependent gene expression through the canonical signaling pathway. Antioxid Redox Signal. 2009; 11:2058–2064.

Pasternack RF, Halliwell B. Superoxide dismutase activities of an iron porphyrin and other iron complexes. J Am Chem Soc. 1979; 101:1026–1031.

Peretz P, Solomon D, Weinraub D, Faraggi M. Chemical properties of water-soluble porphyrins: 3. The reaction of superoxide radicals with some metalloporphyrins. Int J Radiat Biol. 1982; 42:449–456.

Pfeiffer S, Schrammel A, Koestling D, Schmidt K, Meyer B. Molecular actions of a Mn(III)Porphyrin SOD mimetic and peroxynitrite scavenger: reaction with nitric oxide and direct inhibition of NO synthase and soluble guanylyl cyclase. Mol Pharmacol. 1998; 53:795–800. [PubMed: 9547373]

Piganelli JD, Flores SC, Cruz C, Koepp J, Young R, Bradley B, Kachadourian R, Batinic-Haberle I, Haskins K. A metalloporphyrin superoxide dismutase mimetic (SOD mimetic) inhibits autoimmune diabetes. Diabetes. 2002; 51:347–355. [PubMed: 11812741]

Pollard JM, Rebouças JS, Durazo A, Kos I, Fike F, Panni M, Gralla EB, Valentine JS, Batinic-Haberle I, Gatti RA. Radio-protective effects of manganese-containing superoxide dismutase mimics on ataxia telangiectasia cells. Free Radic Biol Med. 2009; 47:250–260. [PubMed: 19389472]

Rabbani Z, Batinic-Haberle I, Anscher MS, Huang J, Day BJ, Alexander E, Dewhirst MW, Vujasković Z. Long term administration of a small molecular weight catalytic metallo-porphyrin antioxidant

AEOL10150 protects lungs from radiation-induced injury. Int J Rad Oncol Biol Phys. 2007a; 67:573–580.

Rabbani Z, Salahuddin FK, Yarmolenko P, Batinic-Haberle I, Trasher BA, Gauter-Fleckenstein B, Dewhirst MW, Anscher MS, Vujasković Z. Low molecular weight catalytic metallo-porphyrin antioxidant AEOL10150 (5 mg/kg) protects rat lungs from fractionated radiation chronic radiation-induced injury. Free Radic Res. 2007b; 41:1273–1282. [PubMed: 17957541]

Rabbani Z, Spasojević I, Zhang X, Moeller BJ, Haberle S, Vasquez-Vivar J, Dewhirst MW, Vujasković Z, Batinic-Haberle I. Antiangiogenic action of redox-modulating Mn(III) *meso*-tetrakis(*N*-ethylpyridinium-2-yl)porphyrin, MnTE-2-PyP^{5+}, via suppression of oxidative stress in a mouse model of breast tumor. Free Radic Biol Med. 2009; 47:992–1004. [PubMed: 19591920]

Rebouças JS, DeFreitas-Silva G, Idemori YM, Spasojević I, Benov L, Batinic-Haberle I. Impact of electrostatics in redox modulation of oxidative stress by Mn porphyrins: Protection of SOD-deficient *Escherichia coli* via alternative mechanism where Mn porphyrin acts as a Mn carrier. Free Radic Biol Med. 2008a; 45:201–210.

Rebouças JS, Spasojević I, Batinic-Haberle I. Pure manganese(III) 5,10,15,20-tetrakis(4-benzoic acid)porphyrin (MnT-BAP) is not a superoxide dismutase mimic in aqueous systems: a case of structure-activity relationship as a watchdog mechanism in experimental therapeutics and biology. J Inorg Biol Chem. 2008b; 13:289–302.

Rebouças JS, Spasojević I, Batinic-Haberle I. Quality of Mn-porphyrin-based SOD mimics and peroxynitrite scavengers for preclinical mechanistic/therapeutic purposes. J Pharm Biomed Anal. 2008c; 48:1046–1049.

Rebouças JS, Kos I, Vujasković Z, Batinic-Haberle I. Determination of residual manganese in Mn porphyrin-based superoxide dismutase (SOD) and peroxynitrite reductase mimics. J Pharm Biomed Anal. 2009; 50:1088–1091. [PubMed: 19660888]

Saba H, Batinic-Haberle I, Munusamy S, Mitchell T, Lichti C, Megyesi J, MacMillan-Crow LA. Manganese porphyrin reduces renal injury and mitochondrial damage during ischemia/reperfusion. Free Radic Biol Med. 2007; 42:1571–1578. [PubMed: 17448904]

Shaulian E, Karin M. AP-1 in cell proliferation and survival. Oncogene. 2001; 20:2390–2400. [PubMed: 11402335]

Sheng H, Yang W, Fukuda S, Tse HM, Paschen W, Johnson K, Batinic-Haberle I, Crapo JD, Pearlstein RD, Piganelli J, Warner DS. Long-term neuroprotection from a potent redox-modulating metalloporphyrin in the rat. Free Radic Biol Med. 2009; 47:917–923. [PubMed: 19631268]

Spasojević I, Batinic-Haberle I. Manganese(III) complexes with porphyrins and related compounds as catalytic scavengers of superoxide. Inorg Chim Acta. 2001; 317:230–242.

Spasojević I, Batinic-Haberle I, Fridovich I. Nitrosylation of manganese(II) tetrakis(*N*-ethylpyridinium-2-yl)porphyrin. Nitric Oxide. 2000; 4:526–533. [PubMed: 11020341]

Spasojević I, Batinic-Haberle I, Stevens RD, Hambright P, Thorpe AN, Grodkowski J, Neta P, Fridovich I. Manganese(III) biliverdin IX dimethylester. A powerful catalytic scavenger of superoxide employing the Mn(III)/Mn(II) redox couple. Inorg Chem. 2001; 40:726–739. [PubMed: 11225116]

Spasojević I, Batinic-Haberle I, Rebouças JS, Idemori YM, Fridovich I. Electrostatic contribution in the catalysis of O2•− dismutation by superoxide dismutase mimics. J Biol Chem. 2003; 278:6831–6837. [PubMed: 12475974]

Spasojević I, Colvin OM, Warshany KR, Batinic-Haberle I. New approach to the activation of anti-cancer pro-drug by metalloporphyrin-based cytochrome P450 mimics in all-aqueous biologically relevant system. J Inorg Biochem. 2006; 100:1897–1902. [PubMed: 16965820]

Spasojević I, Yumin C, Noel T, Yu I, Pole MP, Zhang L, Zhao Y, St Clair DK, Batinic-Haberle I. Mn porphyrin-based SOD mimic, MnTE-2-PyP^{5+} targets mouse heart mitochondria. Free Radic Biol Med. 2007; 42:1193–1200. [PubMed: 17382200]

Spasojević I, Chen Y, Noel TJ, Fan P, Zhang L, Rebouças JS, St Clair DK, Batinic-Haberle I. Pharmacokinetics of the potent redox modulating manganese porphyrin, MnTE-2-PyP^{5+} in plasma and major organs of B6C3F1 mice. Free Radic Biol Med. 2008; 45:943–949. [PubMed: 18598757]

Sun HL, Liu YN, Huang YT, Pan SL, Huang DY, Guh JH, Lee FY, Kuo SC, Teng CM. YC-1 inhibits HIF-1 expression in prostate cancer cells: contribution of Akt/NF-κB signaling to HIF-1α accumulation during hypoxia. Oncogene. 2007; 26:3941–3951. [PubMed: 17213816]

Tauskela JS, Brunette E. Neuroprotection against staurosporine by metalloporphyrins independent of antioxidant capability. Neurosci Lett. 2009; 466:41–46. [PubMed: 19766169]

Tauskela JS, Brunette E, O'Reilly N, Mealing G, Comas T, Gendron TF, Monette R, Morley P. An alternative Ca^{2+}-dependent mechanism of neuroprotection by metalloporphyrin class of superoxide dismutase mimetics. FASEB J. 2005; 19:1734–1736. [PubMed: 16081500]

Toledano MB, Ghosh D, Rinh F, Leonard WJ. *N*-terminal DNA-binding domains contribute to differential DNA-binding specificities of NF-κB p50 and p65. Mol Cellul Biol. 1993; 13:852–860.

Trachootham D, Alexandre J, Huang P. Targeting cancer cells by ROS-mediated mechanisms: a radical therapeutic approach? Nat Rev. 2009; 8:579–591.

Tse HM, Josephy SI, Chan ED, Fouts D, Cooper AM. Activation of the mitogen-activated protein kinase signaling pathway is instrumental in determining the ability of *Mycobacterium avium* to grow in murine macrophages. J Immunol. 2002; 168:825–833. [PubMed: 11777978]

Tse H, Milton MJ, Piganelli JD. Mechanistic analysis of the immunomodulatory effects of a catalytic antioxidant on antigen-presenting cells: Implication for their use in targeting oxidation/reduction reactions in innate immunity. Free Radic Biol Med. 2004; 36:233–247. [PubMed: 14744635]

Vance CK, Miller AF. A simple proposal that can explain the inactivity of metal-substituted superoxide dismutases. J Am Chem Soc. 1998; 120:461–467.

Vujasković Z, Batinic-Haberle I, Rabbani ZN, Feng Q-F, Kang SK, Spasojević I, Samulski TV, Fridovich I, Dewhirst MW, Anscher MS. A small molecular weight catalytic metalloporphyrin antioxidant with superoxide dismutase (SOD) mimetic properties protects lungs from radiation-induced injury. Free Radic Biol Med. 2002; 33:857–863. [PubMed: 12208373]

Warner, DS.; Batinic-Haberle, I.; Sheng, H. Mn porphyrins and stroke. 6th international conference on porphyrins and phthalocyanines; New Mexico. 2010.

Ye X, Fels D, Dedeugd C, Dewhirst MW, Leong K, Batinic-Haberle I. The in vitro cytotoxic effects of Mn(III) alkylpyridylpor-phyrin/ascorbate system on four tumor cell lines. Free Radic Biol Med. 2009; 47:S136.

Yu, L.; Ji, X.; Derrick, M.; Drobyshevsky, A.; Liu, T.; Batinic-Haberle, I.; Tan, S. Testing new porphyrins in in vivo model system: effect of Mn porphyrins in animal model of cerebral palsy. 6th international conference on porphyrins and phthalocyanines; New Mexico. 2010.

Zhao Y, Xue Y, Oberley TD, Kiningham KK, Lin SM, Yen HC, Majima H, Hines J, St Clair D. Overexpression of manganese superoxide dismutase suppresses tumor formation by modulation of activator protein-1 signaling in a multistage skin carcinogenesis model. Cancer Res. 2001; 61:6082–6088. [PubMed: 11507057]

Zhao Y, Chaiswing L, Oberley TD, Batinic-Haberle I, St Clair W, Epstein CJ, St Clair D. A mechanism-based antioxidant approach for the reduction of skin carcinogenesis. Cancer Res. 2005; 65:1401–1405. [PubMed: 15735027]

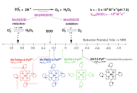

Fig. 1.
Design of Mn porphyrins based on thermodynamic considerations

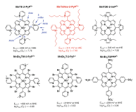

Fig. 2.

Three most often in vivo studied *ortho* isomeric Mn(III) *meso*-tetrakis(*N*-ethyl(or *n*-hexyl)pyridinium-2-yl)porphyrins, MnTE-2-PyP^{5+} (AEOL10113), MnTnHex-2-PyP^{5+}, and the *N*,*N*′-diethylimi-dazolium analog, MnTDE-2-ImP^{5+} (AEOL10150). The *meso* and *beta* positions on porphyrin ring are indicated as well as *ortho*, *meta*, and *para* positions of pyridyl nitrogens with respect to porphyrin *meso* positions. Also shown are three Mn porphyrins that are both *meso*- and *beta*-substituted. Such compounds are particularly valuable tool for the design of perspective therapeutics

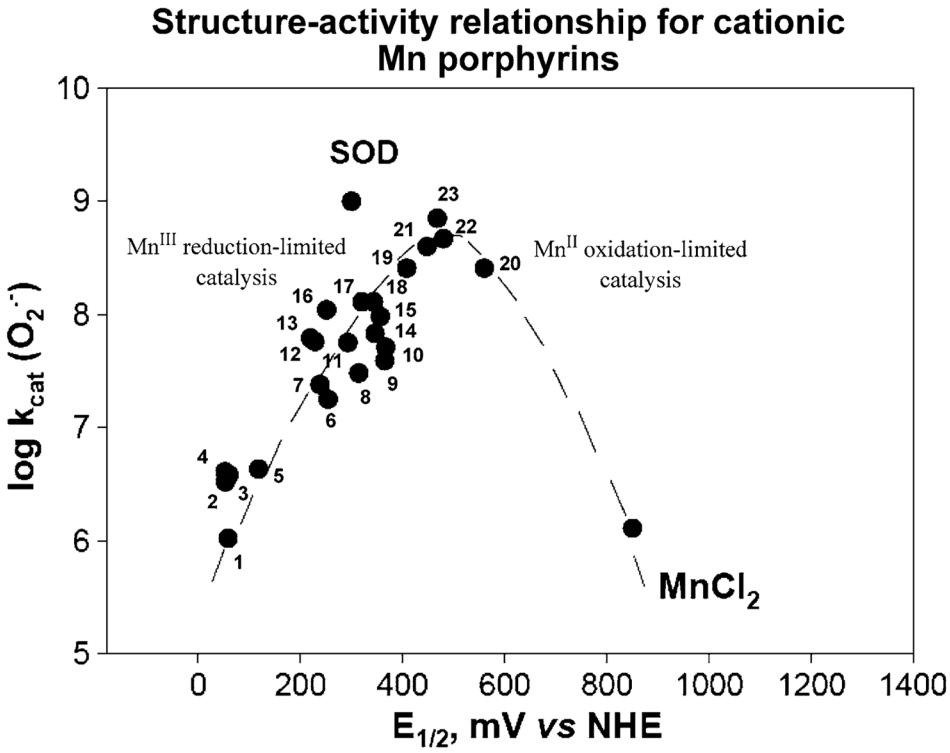

Fig. 3.

Structure–activity relationship between log$k_{cat}(O_2^{\bullet -})$ and $E_{1/2}$ ($Mn^{III}P/Mn^{II}P$) in mV versus NHE for cationic Mn(III) porphyrins. Compounds at the plateau of the *bell-shaped curve* are those that bear both *meso* and *beta* substituents and have highest k_{cat}. Yet, they are stabilized in Mn +2 oxidation state, lose readily Mn and are thus are only important for mechanistic purposes. The falling limb of the *bell-shaped curve* is more obvious in SARs of anionic and neutral porphyrins (Batinic-Haberle et al. 2010). Compounds are: *1* MnT(TFTMA)P^{5+}, *2* MnBM-2-PyP^{5+}, *3* MnTM-4-PyP^{5+}, *4* MnTM-3-PyP^{5+}, *5* MnTrM-2-PyP^{5+}, *6* MnTnBu-2-PyP^{5+}, *7* MnTnPr-2-PyP^{5+}, *8* MnTnHex-2-PyP^{5+}, *9* MnTDMOE-2-ImP^{5+}, *10* MnTnOct-2-PyP^{5+}, *11* MnClTE-2-PyP^{5+}, *12* MnTE-2-PyP^{5+}, *13* MnTM-2-PyP^{5+}, *14* MnTDE-2-ImP^{5+}, *15* MnTM,MOE-2-ImP^{5+}, *16* MnTMOE-2-PyP^{5+}, *17* MnTDM-2-ImP^{5+}, *18* $MnCl_2$TE-2-PyP^{5+}, *19* $MnCl_3$TE-2-PyP^{5+}, *20* $MnCl_5$TE-2-PyP^{5+}, *21* $MnCl_4$TE-2-PyP^{5+}, *22* $MnBr_8$TM-4-PyP^{4+}, and *23* $MnBr_8$TM-3-PyP^{4+}. Data are taken from Batinic-Haberle et al. (2010) and Kachadourian et al. (1998). The names of porphyrins are listed in the list of abbreviations

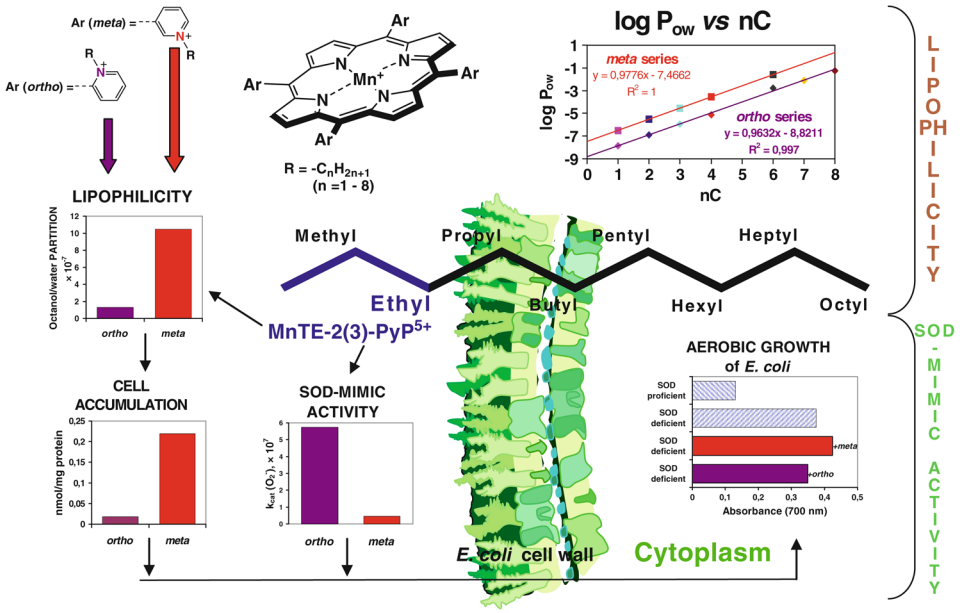

Fig. 4.

Lipophilicity of MnPs increases tenfold by either (1) lengthening alkyl chains by each additional carbon atom, or (2) shifting alkyl groups from *ortho* (2) to *meta* 5 positions. The tenfold increased lipohilicity of *meta* ethyl analog, MnTE-3-PyP^{5+}, resulted in its tenfold higher accumulation in the cytosol of *E. coli* as compared to *ortho* isomer, MnTE-2-PyP^{5+}. Such enhanced accumulation compensated for a tenfold lower ability of MnTE-3-PyP^{5+} to dismute $O_2^{\bullet-}$. In turn both isomers were equally able to substitute for the lack of cytosolic Cu,ZnSOD when *E. coli* grew in aerobic medium (Kos et al. 2009a, b)

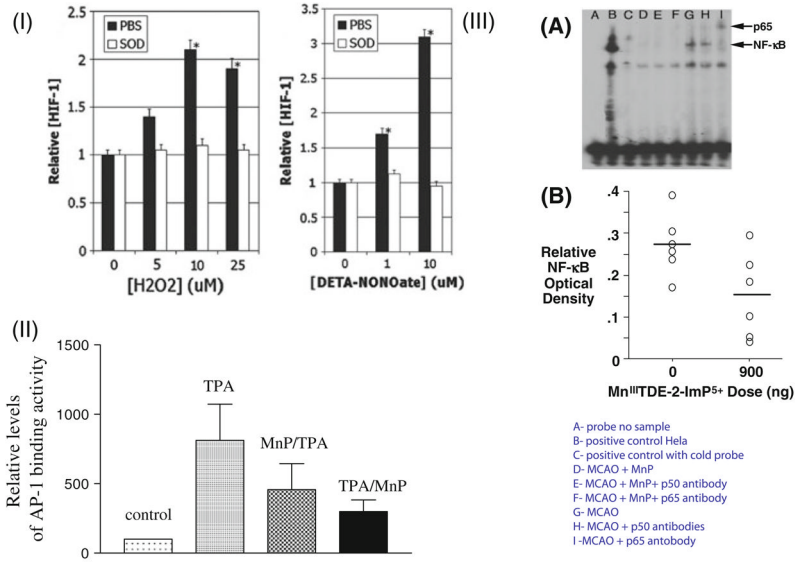

Fig. 5.

MnP prevents activation of redox-active cellular transcription factors. In an in vitro 4T1 mouse breast cancer cell study, HIF-1α was activated by H_2O_2 and nitric oxide but blocked with equimolar concentrations of MnTE-2-PyP^{5+}, indicated in *I* as SOD (Moeller et al. 2004). In *II*, the AP-1 activation in a mouse skin cancerogenesis model was inhibited with MnTE-2-PyP^{5+} given at 5 ng daily for 5 days a week for 4 weeks (Zhao et al. 2005), while in *III*, in a rat stroke 90-min middle cerebral artery (MCAO) occlusion model, the NF-κB activation at 6 h post-MCAO was inhibited with imidazolyl analog, MnTDE-2-ImP^{5+}, given for 1 week intracerebroventricularly (ICV) at 900 ng bolus dose + 56 ng/h ICV infusion for a week starting at 90 min after 90-min MCAO (Sheng et al. 2009)

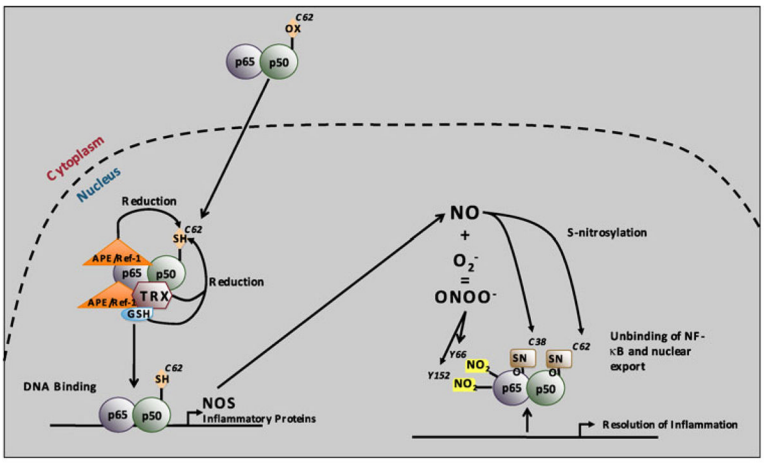

Fig. 6.

Redox-regulation of NF-*κ*B DNA-binding. In resting cells, NF-*κ*B is predominantly found in the cytoplasm of the cell, with an oxidized p50 cysteine 62. Upon activation, NF-*κ*B translocates into the nucleus where p50 cysteine 62 is reduced by APE1/Ref-1, thereby allowing NF-*κ*B DNA binding. APE1/Ref-1 can both act as a redox factor by directly reducing p50 or as a redox chaperone by promoting the reduction of p50 by TRX or GSH. NF-*κ*B DNA binding leads to •NO synthase (NOS) expression, thereby leading to nitric oxide (•NO) production. •NO can in turn modify p50 cysteine 62 and p65 cysteine 38 by *S*-nitrosylation, which unbinds NF-*κ*B from the DNA and contributes to the resolution of inflammation. •NO can also react with $O_2^{\bullet -}$ to generate $ONOO^-$. $ONOO^-$ induces tyrosine nitration of p65 on tyrosine 66 and tyrosine 152, thereby leading to its association with I*κ*B*α* for nuclear export. Copy rights obtained to use Fig. 7 from Gloire and Piette (Antioxid Redox Signal, 11:2209–2222, 2009)

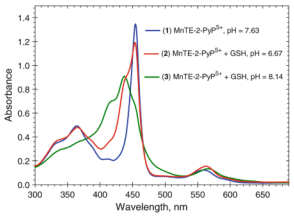

Fig. 7.

The pH-dependent reduction of MnTE-2-PyP^{5+} with gluta-thione. Spectra were taken in 0.1 M tris buffer with 10 μM MnTE-2-PyP^{5+} and 0.7 mM glutathione. The pH values were: 7.63 (*1*), 6.67 (*2*), and 8.14 (*3*). Spectra were taken at 1 min after the reaction had started. The Mn^{III}TE-2-PyP^{5+} has the absorbance at 454 nm (spectrum *1*) (Batinic-Haberle et al. 2002) and the reduced porphyrin Mn^{II}TE-2-PyP^{4+} at 438.4 nm (spectrum *3*) (Spasojevic et al. 2000). The appearance of the shoulder at ~415 nm of the metal-free ligand (Batinic-Haberle et al. 2002) in spectrum *3* suggests that upon reduction a loss of Mn occurs to some extent. At higher pH > 9, GSH is predominantly in a form of more reactive thiolate species in solution. The reaction of MnP with GSH at higher pH may resemble the in vivo conditions where protein cysteines have presumably lower pK_a values (Hill et al. 2009)

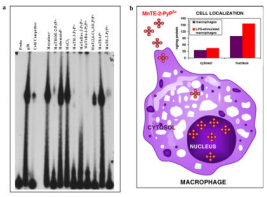

Fig. 8.

a The electrophoretic mobility shift assay (EMSA) of NF-κB in the presence of several different anionic and cationic Mn porphyrins, $Mn(salen)^{+}$ (EUK-8) and $MnCl_2$. The procedure was done as previously described (Tse et al. 2004). In brief, EMSAs with recombinant human NF-κB p50 (Promega) were performed in a cell-free system with the addition of anionic and cationic Mn porphyrins directly in the binding reaction for 15 min prior to the addition of ^{32}P-labeled NF-κB consensus oligo. The following final concentrations of Mn porphyrins were added to the binding reaction: 13.5 μM $Mn(salen)^{+}$, 11 μm MnTMOE-2-PyP^{5+}, 21.3 μM MnhematoP^{-}, 10 μM $MnCl_2$, 9.7 μM MnTM-3-PyP^{5+}, 11.7 μM MnTnHex-2-PyP^{5+}, 11 μM MnTnBu-2-PyP^{5+}, 7.6 μM MnT (2,6-Cl_2-3-SO_3P)P^{3-}, 11 μM $MnTBAP^{3-}$, and 14.3 μM MnTE-2-PyP^{5+}. Protein and DNA complexes were separated on a non-denaturing polyacrylamide gel and identified by autoradiography. **b** Unstimulated and LPS-stimulated macrophages were treated with 34 μM MnTE-2-PyP^{5+} for 1.25 h as described elsewhere (Tse et al. 2002). Using HPLC/fluorescence methodology (Spasojevic et al. 2008), the levels of MnP in the cytosol of unstimulated and LPS-stimulated macrophages were 35 and 44 ng/mg protein, respectively, while in the nucleus, the levels of MnP observed were 99 and 156 ng/mg protein, respectively. The study proved that MnTE-2-PyP^{5+} accumulates more readily in nucleus than in cytosol during macrophage activation

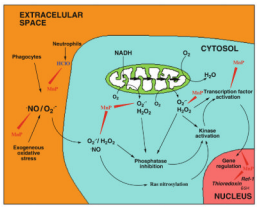

Fig. 9.

Mn porphyrins protect biomolecules by scavenging a variety of ROS/RNS, whereby eliminating a signal for transcription factors activation; such actions occur likely in cytosol. In addition to this antioxidant action, the data by Piganelli group strongly supports the notion that Mn porphyrins in nucleus act as pro-oxidants preventing p50 DNA binding. The drawing was inspired by McCord (2000) publication

Table 1

The k_{cat} for $O_2^{\bullet-}$ dismutation, k_{red} for $ONOO^-$ reduction, $E_{1/2}$, Mn^{III}/Mn^{II}, and lipophilicity expressed as partition between *n*-octanol and water, P_{OW} for Mn(III) porphyrins and few other compounds for comparison purposes

Mn compounds	log k_{cat} ($O_2^{\bullet-}$)	log k_{red} ($ONOO^-$)	$E_{1/2}$ (mV versus NHE)	P_{OW} ($Mn^{III}P$)
$MnTE\text{-}2\text{-}PyP^{5+}$	7.76[a]	7.53[i]	+228[a]	−6.89[n]
$MnTnBu\text{-}2\text{-}PyP^{5+}$	7.25[b]	7.11[i]	+254[b]	−5.11[n]
$MnTnHex\text{-}2\text{-}PyP^{5+}$	7.48[b]	7.11[i]	+314[b]	−2.76[n]
$MnTnOct\text{-}2\text{-}PyP^{5+}$	7.71[b]	7.15[i]	+367	−1.24[n]
$MnTMOE\text{-}2\text{-}PyP^{5+}$	8.04[c]	7.36[k]	+251[m]	~−6.53[o]
$MnTM\text{-}3\text{-}PyP^{5+}$	6.61[d]	6.62[j]	+52[d]	−6.96[n]
$MnTE\text{-}3\text{-}PyP^{5+}$	6.65[n]		+54[n]	−5.98[n]
$MnTDE\text{-}2\text{-}ImP^{5+}$	7.83[c]	7.43[k]	+346[m]	~−6.48[o]
$MnBr_8TM\text{-}3\text{-}PyP^{4+}$	≥8.85[r]		+468[r]	
$MnT(2,6\text{-}Cl_2\text{-}3\text{-}SO_3P)P^{3-}$	6.00[a]		+88[a]	
$MnBr_8TSPP^{3-}$	5.56[f]		+209[f]	
$Mn(hematoP)^-$	~3.00[e]		−230[a]	
$MnTBAP^{3-}$	<3.50[f]	5.02[l]	−194[f]	
$MnT\text{-}2\text{-}PyP^+$	4.29[p]		−280[p]	
$MnT\text{-}4\text{-}PyP^+$	4.53[p]		−200[p]	
$Mn(salen)^+$ (EUK-8)	5.78[g]		−100[g]	
$MnCl_2$	6.1–7.7[h]		+850[q]	
Cu,ZnSOD	~9[f]	3.97[l]	~+300[f]	

[a] Batinic-Haberle et al. (1999)

[b] Batinic-Haberle et al. (2002)

[c] Batinic-Haberle et al. (2004)

[d] Batinic-Haberle et al. (1998)

[e] Estimate based on $E_{1/2}$

[f] Rebouças et al. (2008a, b, c)

[g] Spasojevic et al. (2001)

[h] Spasojevic et al. (2001), Rebouças et al. (2008a, b, c), Barnese et al. (2008), and Archibald and Fridovich (1982)

[i] Ferrer-Sueta et al. (2003)

[j] Ferrer-Sueta et al. (1999)

[k] Determined at 25°C, pH 7.32, then recalculated to 37°C using $MnTE\text{-}2\text{-}PyP^{5+}$ as a reference (Ferrer-Sueta et al., unpublished)

[l] Batinic-Haberle et al. (2009a, b)

[m] Batinic-Haberle et al. (2004)

[n] Kos et al. (2009a)

[o] Estimated from P_{OW} versus R_f plot for *ortho* Mn(III) *N*-alkylpyridylporphyrins based on TLC R_f values from Batinic-Haberle et al. (2004)

[p] Spasojevic and Batinic-Haberle (2001)

[q] Spasojevic and Batinic-Haberle (2001), oxidation potential only, Mn^{II}/Mn^{III} redox couple is irreversible

[r] DeFreitas-Silva et al. (2008)